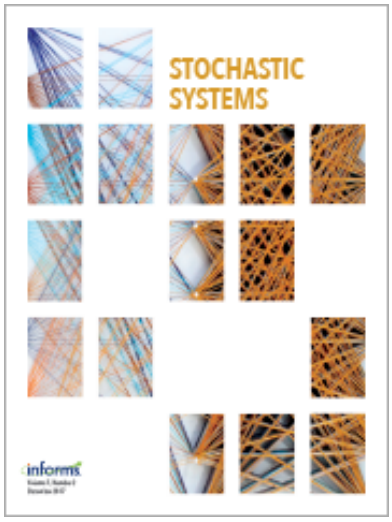

Stochastic Systems

Publication details, including instructions for authors and subscription information:
http://pubsonline.informs.org

A Two-dimensional, Two-sided Euler Inversion Algorithm with Computable Error Bounds and its Financial Applications

Ning Cai, Chao Shi

To cite this article:
Ning Cai, Chao Shi (2014) A Two-dimensional, Two-sided Euler Inversion Algorithm with Computable Error Bounds and its Financial Applications. Stochastic Systems 4(2):404-448. https://doi.org/10.1287/12-SSY094

Stochastic Systems
2014, Vol. 4, No. 2, 404–448
DOI: 10.1214/12-SSY094

A TWO-DIMENSIONAL, TWO-SIDED EULER INVERSION ALGORITHM WITH COMPUTABLE ERROR BOUNDS AND ITS FINANCIAL APPLICATIONS

By Ning Cai* and Chao Shi†

*The Hong Kong University of Science and Technology** *and University of International Business and Economics*†

In this paper we propose an inversion algorithm with computable error bounds for two-dimensional, two-sided Laplace transforms. The algorithm consists of two discretization parameters and two truncation parameters. Based on the computable error bounds, we can select these parameters appropriately to achieve any desired accuracy. Hence this algorithm is particularly useful to provide benchmarks. In many cases, the error bounds decay quickly (e.g., exponentially), making the algorithm very efficient. We apply this algorithm to price exotic options such as spread options and barrier options under various asset pricing models as well as to evaluate the joint cumulative distribution functions of related state variables. The numerical examples indicate that the inversion algorithm is accurate, fast and easy to implement.

1. Introduction It is well-known that European option prices under the Black-Scholes model (BSM) can be computed directly via the celebrated Black-Scholes formula. However, closed-form solutions for European option prices are usually unavailable in more sophisticated asset pricing models. Carr and Madan [9] applied the fast Fourier transform (FFT) method to value European options under a wide range of models. Specifically, if the characteristic function of the asset return is known analytically, one can derive a closed-form, one-dimensional Fourier transform for the European option value with respect to (w.r.t.) the logarithm of the strike price. Then the FFT can be used to invert this one-dimensional Fourier transform to produce a numerical European option price. For more related literature, we refer to Carr and Madan [9, 10] and references therein.

However, as pointed out in [10], the plain FFT breaks down for deep out of the money options and even generates negative values. This problem becomes more serious for model calibration which requires us to value

Received January 2013.
AMS 2000 subject classifications: 44A10, 91G20, 91G60.
Keywords and phrases: Two-dimensional Laplace inversion, two-sided Laplace transforms, Euler inversion, computable error bounds, discretization errors, truncation errors, option pricing, exotic options.

European options for a wide spectrum of strikes repeatedly. Indeed, even in the cases when Carr and Madan's FFT breaks down, its accuracy can be improved by making different choices of the algorithm parameters. For example, Lee [21] studied how to improve the accuracy of one-dimensional Fourier transform method by conducting an error analysis. Alternatively, in the framework of Euler inversion algorithms, Cai et al. [7] generalized the elegant Euler inversion algorithm for one-sided Laplace transforms (Abate and Whitt [1]) to the two-sided case, and the computable error bounds of the resulting algorithm enable us to select the parameters suitably to achieve desired accuracy.

It is worth noting that these inversion algorithms are focused on one-dimensional transforms, which are available in closed form for European options in a wide range of models. Nonetheless, for many exotic options even under simple models, there exist only closed-form solutions to two-dimensional (two-sided) Laplace transforms rather than one-dimensional (one-sided) ones; e.g., barrier options and step options under the double- and mixed-exponential jump diffusion models, and spread options under the variance gamma model and even under the BSM.

In this paper, we propose an inversion algorithm with *computable error bounds* for two-dimensional, two-sided Laplace transforms. Although an important motivation of ours is to price exotic options in financial engineering, the developed algorithm is much more widely applicable and can be potentially used to compute quantities of interest in general contexts with known two-dimensional Laplace transforms, e.g., the time-dependent probability distributions in queueing models (see Choudhury et al. [11]), the operational solutions of fractional diffusion equations (see Valkó and Abate [26]), and the first passage time distributions for spectrally one-sided Lévy processes (see Rogers [24]). The algorithm has three appealing features.

(i) The Laplace inversion formula is very simple to implement (see (5)), involving four parameters—two discretization parameters C_1 and C_2 and two truncation parameters N_1 and N_2.

(ii) Both discretization and truncation errors have explicit expressions. As a result, under mild conditions we can derive *computable bounds* for both errors in terms of parameters C_1, C_2, N_1 and N_2. By choosing these parameters appropriately based on computable error bounds, the algorithm can achieve any desired accuracy, and therefore is especially useful to provide benchmarks.

(iii) In many cases, the discretization error bound decays exponentially, while the truncation error bound decays exponentially or in a power law, leading to fast computation.

Our algorithm essentially extends the one-dimensional, two-sided Laplace inversion algorithm in [7] to the two-dimensional case. Another key difference between these two papers is that we provide a unified approach to finding the discretization error bounds based on the "known" Laplace transforms rather than the "unknown" original functions; see Section 3.2.1 and Proposition 3.2. This technique can also be applied to the one-dimensional case.

Our algorithm can also be viewed as an extension of the multidimensional, one-sided Euler inversion algorithm in [11] to the two-sided case. Petrella [23] proposed a similar algorithm with a scaling factor but without rigorous justification. As pointed out in [7], Petrella's method imposed a constraint on the scaling parameter, which may cause large errors even in the one-dimensional case; see Section 4.3 in [7]. Furthermore, Petrella did not analyze the truncation errors. Lee [21] conducted an elegant error analysis for the one-dimensional Fourier transform method. By contrast, our paper deals with the so-called Euler inversion algorithm in the *two-dimensional* case, where the inversion formula and hence the expressions of discretization and truncation errors are different. Therefore, the error analysis especially for discretization errors is also different.

In fact, our algorithm essentially belongs to the category of Euler inversion algorithms which have enjoyed great popularity in the areas of operations research and applied probability (see, e.g., [1, 11, 23, 7]). Motivated by applications in financial engineering, e.g., path-dependent option pricing, we extend the existing Euler inversion algorithms to the two-dimensional, two-sided case. An attractive feature of our algorithm is that in many cases, we can derive *computable bounds* for both discretization and truncation errors (please see Sections 5–7). As a result, the numerical outputs of our algorithm consist of not only the inversion result but also the two error bounds (please see the numerical results in Section 8). These error bounds can tell us how accurate our inversion results are. This is useful especially in the absence of reliable benchmarks. Furthermore, by choosing the algorithm parameters appropriately based on the computable error bounds, we can achieve any desired accuracy. Therefore, our algorithm is particularly useful to provide benchmarks.

Besides Fourier and Laplace transforms, other transform-based methods applied in financial engineering include the Hilbert transform in Feng and Linetsky [13, 14], the sinc expansion in Feng and Lin [12], and the fast Gaussian transform in Broadie and Yamamoto [2], to name just a few. These algorithms serve different purposes. For example, the Hilbert transform method is a powerful instrument to calculate expectations involving indicator functions. The sinc expansion approach along with the Hilbert transform is very

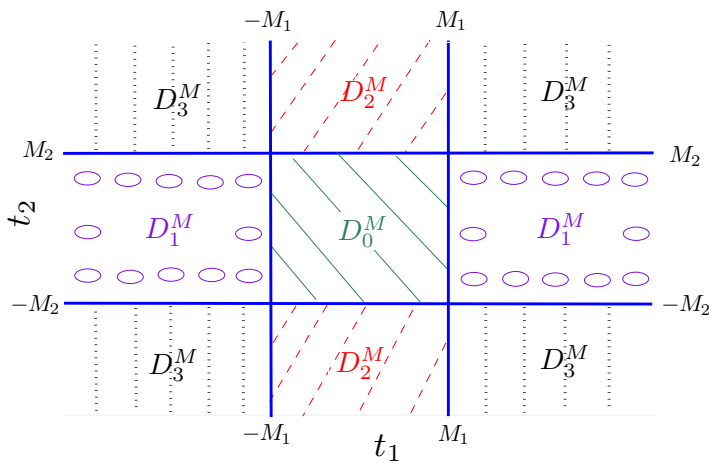

FIG 1. *Divide the plane into four disjoint regions w.r.t.* $\vec{M} = (M_1, M_2)$.

accurate, efficient, and robust in evaluating the cumulative distribution function (cdf) of the asset return and in pricing European options under exponential Lévy models. The fast Gaussian transform algorithm is extremely fast and especially useful when pricing discrete barrier and lookback options under models with Gaussian or mixed-Gaussian returns.

The remainder of this paper is organized as follows. Section 2 presents the two-dimensional, two-sided Laplace inversion formula. We investigate the bounds for discretization and truncation errors in Sections 3 and 4, respectively. The financial applications of our inversion algorithm are discussed in Sections 5–7, and numerical results are given in Section 8. All the proofs are deferred to the appendices.

2. The main result Before presenting our main result, we introduce several notations used throughout the paper. $\vec{x}$ denotes a two-dimensional row vector $(x_1, x_2) \in \mathbb{R}^2$ or $\mathbb{C}^2$. For any $\vec{x}$ and $\vec{y}$, their inner product and Hadamard product are expressed by "$\cdot$" and "$\circ$", respectively, i.e.,

$$\vec{x} \cdot \vec{y} := x_1 y_1 + x_2 y_2 \qquad \text{and} \qquad \vec{x} \circ \vec{y} := (x_1 y_1, x_2 y_2).$$

For ease of exposition, we divide the plane $\mathbb{R}^2$ into the following four disjoint regions w.r.t. $\vec{M} = (M_1, M_2)$; see Figure 1 for an illustration.

$$D_0^{\vec{M}} = \{\vec{t} : |t_1| \le M_1, |t_2| \le M_2\}, \qquad D_1^{\vec{M}} = \{\vec{t} : |t_1| > M_1, |t_2| \le M_2\},$$
$$D_2^{\vec{M}} = \{\vec{t} : |t_1| \le M_1, |t_2| > M_2\}, \qquad D_3^{\vec{M}} = \{\vec{t} : |t_1| > M_1, |t_2| > M_2\}.$$

2.1. *Two-dimensional, two-sided Laplace transforms* Consider a function $f(\vec{t})$ defined for $\vec{t} \equiv (t_1, t_2) \in \mathbb{R}^2$. Its *two-sided Laplace transform* or *bilateral Laplace transform* $L_f(\vec{s})$ is defined as

$$L_f(\vec{s}) := \int_{-\infty}^{+\infty} \int_{-\infty}^{+\infty} e^{-\vec{s}\cdot\vec{t}} f(\vec{t}) dt_1 dt_2 \tag{1}$$

for complex vector $\vec{s} \equiv \vec{v} + i\vec{\omega} \in \mathbb{C}^2$, where $\vec{v} \equiv \Re(\vec{s})$ and $\vec{\omega} \equiv \Im(\vec{s})$ are real and imaginary parts of $\vec{s}$, respectively. We define the *region of absolute convergence (ROAC)* of the two-sided Laplace transform to be the interior of the following set

$$\left\{ \vec{s} \in \mathbb{C}^2 : \int_{-\infty}^{+\infty} \int_{-\infty}^{+\infty} |e^{-\Re(\vec{s})\cdot\vec{t}} f(\vec{t})| dt_1 dt_2 < +\infty \right\}. \tag{2}$$

It is easy to see that $L_f(\vec{s})$ in (1) is well defined for any $\vec{s} \in$ROAC.

Note that the ROAC does not depend upon $\Im(\vec{s})$. Therefore, we can simply use the range of $\Re(\vec{s})$ to represent the ROAC throughout the paper.

We point out that both two-dimensional, one-sided Laplace transforms and two-dimensional Fourier transforms are special cases of two-dimensional, two-sided Laplace transforms. Indeed, if $f(\vec{t}) = 0$ for any $\vec{t} \notin [0, +\infty) \times [0, +\infty)$, then its two-sided Laplace transform is reduced to the one-sided one

$$L_f(\vec{s}) = \int_0^{+\infty} \int_0^{+\infty} e^{-\vec{s}\cdot\vec{t}} f(\vec{t}) dt_1 dt_2, \qquad \text{for } \Re(\vec{s}) \in \text{ROAC}.$$

If we confine our attention to $L_f(\vec{s})$ only for $\vec{s}$ with $\Re(\vec{s}) = 0$, this results in the *Fourier transform* $\mathcal{F}_f(\vec{\omega})$ of the function $f(\vec{t})$

$$\mathcal{F}_f(\vec{\omega}) := \int_{-\infty}^{\infty} \int_{-\infty}^{\infty} e^{-i\vec{\omega}\cdot\vec{t}} f(\vec{t}) dt_1 dt_2 \equiv L_f(i\vec{\omega}), \qquad \text{for any } \vec{\omega} \in \mathbb{R}^2.$$

It is worth noting that the ROACs of certain two-sided Laplace transforms may not include the imaginary axis. Thus the corresponding Fourier transforms might not be well defined.

2.2. *The two-dimensional, two-sided Laplace inversion formula* Under mild conditions, we shall derive a two-dimensional, two-sided Laplace inversion formula that involves the parameters $\vec{C} = (C_1, C_2)$ and $\vec{N} = (N_1, N_2)$ for the purpose of controlling discretization and truncation errors, respectively.

ASSUMPTION 2.1. The function $f(\vec{t})$ is continuous on $\mathbb{R}^2$, and for any fixed $\vec{v} \in \text{ROAC}$ of $L_f(\cdot)$, the function $g(\vec{t}) := e^{-\vec{v}\cdot\vec{t}} f(\vec{t})$ has the following upper bound:

$$|g(\vec{t})| \le \kappa e^{-c_1|t_1|-c_2|t_2|}, \tag{3}$$

where κ, c_1, and c_2 are positive constants independent of $\vec{t}$.

ASSUMPTION 2.2. For any fixed $\vec{v} \in \text{ROAC}$, there exists a constant $\alpha > 1$ such that

(i) for any fixed ω_2, $|L_f(\vec{v} + i\vec{\omega})| = \mathrm{O}(|\omega_1|^{-\alpha})$ as $|\omega_1| \to +\infty$;
(ii) for any fixed ω_1, $|L_f(\vec{v} + i\vec{\omega})| = \mathrm{O}(|\omega_2|^{-\alpha})$ as $|\omega_2| \to +\infty$; and
(iii) $|L_f(\vec{v} + i\vec{\omega})| = \mathrm{O}(|\omega_1\omega_2|^{-\alpha})$ as $|\omega_1|, |\omega_2| \to +\infty$.

THEOREM 2.3. *Consider a function $f(\vec{t})$ satisfying Assumption 2.1 and 2.2. Then for any $\vec{v} \in ROAC$, $\vec{t} \in \mathbb{R}^2$, $\vec{C} \ge 0$, and $\vec{N} \in \mathbb{N}^2$ such that $(|t_1| + C_1)(|t_2| + C_2) \ne 0$, we have*

$$f(\vec{t}) = f_A(\vec{t}, \vec{v}, \vec{C}, \vec{N}) + e_T(\vec{t}, \vec{v}, \vec{C}, \vec{N}) - e_D(\vec{t}, \vec{v}, \vec{C}). \tag{4}$$

(I) $f_A(\vec{t}, \vec{v}, \vec{C}, \vec{N})$ is an approximation to $f(\vec{t})$ and is given by

(5)
$$f_A(\vec{t}, \vec{v}, \vec{C}, \vec{N}) = \frac{e^{\vec{v}\cdot\vec{t}}}{4(|t_1| + C_1)(|t_2| + C_2)} \times \sum_{\vec{k} \in \mathbb{Z}^2 \cap D_0^{\vec{N}}} (-1)^{k_1+k_2} \Re\left(e^{-i(\vec{a}\circ\vec{k}\circ\vec{C})\cdot sgn(\vec{t})} L_f(\vec{v} + i\vec{a}\circ\vec{k})\right),$$

where $sgn(x)$ equals 1 if $x \ge 0$ and -1 otherwise, $sgn(\vec{t}) := (sgn(t_1), sgn(t_2))$, and $a_j = \frac{\pi}{t_j + C_j\, sgn(t_j)}$ for $j = 1, 2$.

(II) $e_T(\vec{t}, \vec{v}, \vec{C}, \vec{N})$ and $e_D(\vec{t}, \vec{v}, \vec{C})$ denote the truncation error and the discretization error of the approximation $f_A(\vec{t}, \vec{v}, \vec{C}, \vec{N})$ to $f(\vec{t})$, respectively.

(6)
$$e_T(\vec{t}, \vec{v}, \vec{C}, \vec{N}) = \frac{e^{\vec{v}\cdot\vec{t}}}{4(|t_1| + C_1)(|t_2| + C_2)} \times \sum_{\vec{k} \in \mathbb{Z}^2 \setminus D_0^{\vec{N}}} (-1)^{k_1+k_2} \Re\left(e^{-i(\vec{a}\circ\vec{k}\circ\vec{C})\cdot sgn(\vec{t})} L_f(\vec{v} + i\vec{a}\circ\vec{k})\right),$$

$$e_D(\vec{t}, \vec{v}, \vec{C}) = \sum_{\vec{k} \in \mathbb{Z}^2 \setminus \{\vec{0}\}} e^{-2(\vec{v}\circ\vec{k})\cdot(\vec{t} + \vec{C}\circ sgn(\vec{t}))} f(\vec{t} + 2\vec{k}\circ(\vec{t} + \vec{C}\circ sgn(\vec{t}))). \tag{7}$$

PROOF. See Appendix A. □

REMARK 2.1. Assumption 2.1 and 2.2 are sufficient but not necessary for the inversion formula (4) to hold. Indeed, they are used to justify a two-dimensional Poisson summation formula in the proof. Other conditions that can validate the Poisson summation formula will also lead to (4). We adopt Assumption 2.1 and 2.2 mainly because they are mild and easy to check in many financial applications.

REMARK 2.2. The inversion algorithm is easy to implement in that the inversion formula (5) is very simple. Furthermore, both discretization and truncation errors have closed-form expressions which facilitate respective error controls. As one shall see later, we can usually control them to achieve any desired accuracy by choosing sufficiently large discretization parameter $\vec{C}$ and truncation parameter $\vec{N}$.

3. Discretization errors

3.1. *Necessity of introducing the discretization parameter* $\vec{C}$ First of all, we point out that to invert the two-sided Laplace transforms, the introduction of the discretization parameter $\vec{C}$ is necessary. Without introducing $\vec{C}$ (i.e., if $\vec{C} = \vec{0}$), the discretization error can be quite large no matter what $\vec{v} \in$ ROAC is selected; see the example below.

Consider evaluating the two-dimensional standard normal probability density function (pdf) $f(\vec{t}) = \frac{1}{2\pi} e^{-\frac{1}{2}(t_1^2+t_2^2)}$ at the point $\vec{t}^* = (\frac{1}{4}, \frac{1}{4})$ by inverting its Laplace transform $L_f(\vec{s}) = e^{\frac{1}{2}(s_1^2+s_2^2)}$ via the two-dimensional, two-sided Laplace inversion algorithm. If $\vec{C} = \vec{0}$, simple algebra yields that the discretization error satisfies

$$e_D(\vec{t}^*, \vec{v}, \vec{0}) \geq \begin{cases} f(-\frac{1}{4}, -\frac{1}{4}) e^{\frac{1}{2}(v_1+v_2)} \geq f(-\frac{1}{4}, -\frac{1}{4}) > 0.14, & \text{if } v_1 \geq 0, v_2 \geq 0; \\ f(\frac{3}{4}, -\frac{1}{4}) e^{\frac{1}{2}(-v_1+v_2)} \geq f(\frac{3}{4}, -\frac{1}{4}) > 0.11, & \text{if } v_1 < 0, v_2 \geq 0; \\ f(-\frac{1}{4}, \frac{3}{4}) e^{\frac{1}{2}(v_1-v_2)} \geq f(-\frac{1}{4}, \frac{3}{4}) > 0.11, & \text{if } v_1 \geq 0, v_2 < 0; \\ f(\frac{3}{4}, \frac{3}{4}) e^{\frac{1}{2}(-v_1-v_2)} \geq f(\frac{3}{4}, \frac{3}{4}) > 0.09, & \text{if } v_1 < 0, v_2 < 0. \end{cases}$$

In other words, no matter what $\vec{v} \in \mathbb{R}^2 \equiv$ ROAC is chosen, the inversion algorithm without the introduction of $\vec{C}$ always leads to a large discretization error (>0.09). See Figure 2 for an illustration. When $\vec{C} = \vec{0}$ and $\vec{v}$ varies in the rectangle $[-1, 1] \times [-1, 1]$, the absolute errors between the true value and the inversion results are no less than 3.6175. However, when $\vec{C}$ increases to $(1.5, 1)$ and then to $(2.5, 3)$, the maximum absolute errors decrease dramatically to 0.2022 and 3.9399×10^{-5}, respectively.

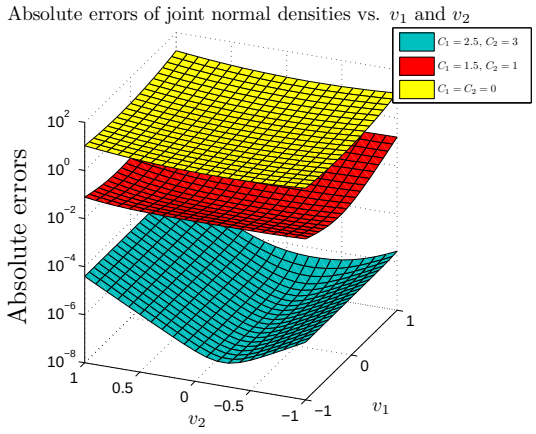

FIG 2. *Absolute errors when evaluating the two dimensional standard normal density at* $\vec{t}^* = \left(\frac{1}{4}, \frac{1}{4}\right)$ *via the two-dimensional, two-sided Laplace inversion algorithm with* $\vec{N} = (200, 200)$ *and* $\vec{C} = (0, 0)$, $(1.5, 1)$, *and* $(2.5, 3)$. *When* $\vec{C} = (0, 0)$, *the minimum absolute error is* 3.6175. *When* $\vec{C}$ *increases to* $(1.5, 1)$ *and* $(2.5, 3)$, *the maximum absolute errors decrease to 0.2022 and* 3.9399×10^{-5}, *respectively.*

3.2. *Exponential decay of discretization errors* Introducing the discretization parameter $\vec{C}$ is not only necessary but can also make the discretization error achieve an exponential decay, leading to a fast computation for the inversion algorithm. When implementing the numerical inversion in practice, we usually first choose a closed rectangle

$$[l_1^*, u_1^*] \times [l_2^*, u_2^*] \subset \text{ROAC}.$$

Without loss of generality, l_j^* and u_j^* for $j = 1, 2$ are assumed to be nonzero. The following theorem shows that for any $\vec{v} \in (l_1^*, u_1^*) \times (l_2^*, u_2^*)$, the discretization error decays exponentially as $\vec{C}$ increases.

THEOREM 3.1. *If there exists a function* $\delta(\cdot)$ *such that for any* $\vec{y} \in [l_1^*, u_1^*] \times [l_2^*, u_2^*]$,

$$e^{-\vec{y}\cdot\vec{t}}|f(\vec{t})| \le \delta(\vec{y}) < +\infty, \quad \textit{for any } \vec{t} \in \mathbb{R}^2, \tag{8}$$

then for any $\vec{v} \in (l_1^*, u_1^*) \times (l_2^*, u_2^*)$, $\vec{C} \in \mathbb{R}_+^2$ *and* $\vec{t} \in \mathbb{R}^2$, *the discretization error has the following bound*

$$|e_D(\vec{t}, \vec{v}, \vec{C})| \le \frac{\rho(\vec{v}, \vec{t})}{(e^{2d_1C_1} - 1)(e^{2d_2C_2} - 1)} + \frac{\rho_1(v_1, t_1)}{e^{2d_1C_1} - 1} + \frac{\rho_2(v_2, t_2)}{e^{2d_2C_2} - 1}, \tag{9}$$

where $d_j = \min\{v_j - l_j^*, u_j^* - v_j\}$ *for j=1,2,*

$$\rho_1(v_1,t_1) = \delta(l_1^*,l_2^*)e^{l_1^*t_1-2(v_1-l_1^*)|t_1|} + \delta(u_1^*,l_2^*)e^{u_1^*t_1-2(u_1^*-v_1)|t_1|},$$

$$\rho_2(v_2,t_2) = \delta(l_1^*,l_2^*)e^{l_2^*t_2-2(v_2-l_2^*)|t_2|} + \delta(l_1^*,u_2^*)e^{u_2^*t_2-2(u_2^*-v_2)|t_2|},$$

and

$$\begin{aligned}\rho(\vec{v},\vec{t}) = {} & \delta(l_1^*,l_2^*)\exp\left\{l_1^*t_1 - 2(v_1-l_1^*)|t_1| + l_2^*t_2 - 2(v_2-l_2^*)|t_2|\right\}\\ & + \delta(u_1^*,l_2^*)\exp\left\{u_1^*t_1 - 2(u_1^*-v_1)|t_1| + l_2^*t_2 - 2(v_2-l_2^*)|t_2|\right\}\\ & + \delta(u_1^*,u_2^*)\exp\left\{u_1^*t_1 - 2(u_1^*-v_1)|t_1| + u_2^*t_2 - 2(u_2^*-v_2)|t_2|\right\}\\ & + \delta(l_1^*,u_2^*)\exp\left\{l_1^*t_1 - 2(v_1-l_1^*)|t_1| + u_2^*t_2 - 2(u_2^*-v_2)|t_2|\right\}.\end{aligned}$$

Moreover, it follows that $\lim_{C_1,C_2\to+\infty} e_D(\vec{t},\vec{v},\vec{C}) = 0$.

PROOF. See Appendix B. □

REMARK 3.1. As interpreted in Section 3.2.1 and illustrated in Sections 5–7, in many cases $\delta(\vec{y})$ in (8) can be specified explicitly. As a result, the upper bound (9) of the discretization error is computable, and hence we can control the discretization error simply by choosing sufficiently large C_1 and C_2.

The choice of $[l_1^*,u_1^*]\times[l_2^*,u_2^*]$ affects the selection of $\vec{C}$ and $\vec{N}$ in a complicated way. Indeed, from (9), we can see that it affects the selection of $\vec{C}$ through $\rho(\vec{v},\vec{t})$, $\rho_1(v_1,t_1)$, $\rho_2(v_2,t_2)$ (where the values of the function $\delta(\vec{y})$ at the four corner points of $[l_1^*,u_1^*]\times[l_2^*,u_2^*]$ are involved) and d_j for $j=1,2$. However, $\delta(\vec{y})$ is specified case by case and could be selected in different ways even in the same case. Therefore, the effect of $[l_1^*,u_1^*]\times[l_2^*,u_2^*]$ on the selection of $\vec{C}$ also depends on the selection of $\delta(\vec{y})$ and might need to be analyzed case by case. Besides, since $[l_1^*,u_1^*]\times[l_2^*,u_2^*]$ affects the selection of $\vec{C}$, (14) and (16) imply that $[l_1^*,u_1^*]\times[l_2^*,u_2^*]$ also affects the selection of $\vec{N}$ through $\zeta_j(\vec{v},k_jb_j\mathrm{sgn}(t_j))$ for $j=1,2$ (here $b_j := \frac{\pi}{|t_j|+C_j}$) as well as through $b_1^{-\alpha_1}$, $b_2^{-\alpha_2}$, $b_1^{-\alpha_3}$ and $b_2^{-\alpha_4}$ in the case of (14) or through $b_1^{\xi_1}$, $b_2^{\xi_2}$, $b_1^{\xi_3}$ and $b_2^{\xi_4}$ in the case of (16). Nonetheless, the functions $\zeta_j(\vec{v},\omega_j)$ and the values of α_j and ξ_j are different if the quantities to compute and/or the models are different. Accordingly, the effect of $[l_1^*,u_1^*]\times[l_2^*,u_2^*]$ on the selection of $\vec{N}$ might also need to be analyzed case by case.

However, it is worth pointing out that although the choice of $[l_1^*,u_1^*]\times[l_2^*,u_2^*]$ affects the selection of $\vec{C}$ and $\vec{N}$, as long as it is selected from the

ROAC, we can always use the discretization and truncation error bounds to achieve the desired accuracy by choosing sufficiently large $\vec{C}$ and $\vec{N}$. Moreover, numerical examples suggest that the resulting algorithms are accurate and fast.

3.2.1. *Specification of the function $\delta(\vec{y})$* To guarantee that Theorem 3.1 holds, we need to specify the function $\delta(\vec{y})$ in (8). However, since this depends on the information about the unknown original function $f(\vec{t})$, it does not seem easy. Sometimes we can specify $\delta(\vec{y})$ based on probability meanings of the unknown function $f(\vec{t})$ in financial applications. This is exactly what is used in Cai et al. [7] in the one-dimensional case. Nonetheless, this problem seems challenging in general cases.

To overcome this difficulty, in Proposition 3.2 we propose a general approach to specifying $\delta(\vec{y})$ based on the *known* Laplace transform $L_f(\vec{y}+i\vec{\omega})$ of $f(\vec{t})$ rather than the *unknown* function $f(\vec{t})$.

PROPOSITION 3.2. *If for any $\vec{y} \in [l_1^*, u_1^*] \times [l_2^*, u_2^*]$, the function $\delta(\vec{y})$ satisfies*

$$\int_{-\infty}^{+\infty}\int_{-\infty}^{+\infty} |L_f(\vec{y}+i\vec{\omega})|d\omega_1 d\omega_2 \le 4\pi^2\delta(\vec{y}), \tag{10}$$

then it also satisfies (8).

PROOF. See Appendix B. □

According to Proposition 3.2, as long as we can find a function $\delta(\vec{y})$ that satisfies (10), then it also satisfies (8). Since $L_f(\vec{y}+i\vec{\omega})$ is assumed to be given in closed form, it is usually easy to explicitly specify $\delta(\vec{y})$ that satisfies (10) and hence (8). Indeed, if we can show that $L_f(\vec{y}+i\vec{\omega})$ satisfies certain asymptotic conditions (13) or (15) and moreover, if we can find $L(\vec{y})$, $L_1(\vec{y})$ and $L_2(\vec{y})$ satisfying (these two conditions are satisfied in many applications; see Sections 5–7)

$$\begin{aligned}&\sup_{|\omega_1|<M_1,|\omega_2|<M_2} |L_f(\vec{y}+i\vec{\omega})| \le L(\vec{y}), \quad \sup_{|\omega_1|\le M_1} |\zeta_1(\vec{y},\omega_1)| \le L_1(\vec{y}), \text{ and}\\ &\sup_{|\omega_2|\le M_2} |\zeta_2(\vec{y},\omega_2)| \le L_2(\vec{y}),\end{aligned} \tag{11}$$

for any $\vec{y} \in$ ROAC, then some simple algebra yields that for any $\vec{y} \in$ ROAC,

$$\int_{-\infty}^{+\infty}\int_{-\infty}^{+\infty} |L_f(\vec{y}+i\vec{\omega})|d\omega_1 d\omega_2 \le 4U(\vec{y}),$$

where $U(\vec{y})$ is defined as

(12)
$$U(\vec{y}) = \begin{cases} M_1 M_2 L(\vec{y}) + \dfrac{M_1 M_2^{\alpha_2 - 1} L_1(\vec{y})}{\alpha_2 - 1} + \dfrac{M_1^{\alpha_1 - 1} M_2 L_2(\vec{y})}{\alpha_1 - 1} \\ \qquad + \zeta(\vec{y}) \dfrac{M_1^{\alpha_3 - 1}}{\alpha_3 - 1} \dfrac{M_2^{\alpha_4 - 1}}{\alpha_4 - 1}, & \text{if (13) holds;} \\ M_1 M_2 L(\vec{y}) + M_1 L_1(\vec{y}) \dfrac{\rho_2^{(\alpha_2 - 1)/\xi_2}}{\xi_2} \Gamma\left(\dfrac{1 - \alpha_2}{\xi_2}, \rho_2 M_2^{\xi_2}\right) \\ \qquad + M_2 L_2(\vec{y}) \dfrac{\rho_1^{(\alpha_1 - 1)/\xi_1}}{\xi_1} \Gamma\left(\dfrac{1 - \alpha_1}{\xi_1}, \rho_1 M_1^{\xi_1}\right) \\ \qquad + \zeta(\vec{y}) \dfrac{\rho_3^{(\alpha_3 - 1)/\xi_3}}{\xi_3} \cdot \dfrac{\rho_4^{(\alpha_4 - 1)/\xi_4}}{\xi_4} \Gamma\left(\dfrac{1 - \alpha_3}{\xi_3}, \rho_3 M_3^{\xi_3}\right) \\ \qquad \times \Gamma\left(\dfrac{1 - \alpha_4}{\xi_4}, \rho_4 M_4^{\xi_4}\right), & \text{if (15) holds.} \end{cases}$$

Then applying Proposition 3.2, we can specify $\delta(\vec{y}) := \pi^2 U(\vec{y})$, which satisfies (8).

As a by-product of Proposition 3.2, we have the following proposition to verify the condition (3) in Assumption 2.1.

PROPOSITION 3.3. *If there exists a function $\delta(\vec{v})$ that satisfies (8) for any $\vec{v}$ in ROAC of $L_f(\vec{s})$, then there exist κ, c_1 and c_2 such that (3) holds.*

PROOF. See Appendix B. □

4. Truncation errors In addition to the discretization error $e_D(\vec{t}, \vec{v}, \vec{C})$, our inversion formula (4) has another error source—the truncation error $e_T(\vec{t}, \vec{v}, \vec{C}, \vec{N})$. In Theorem 4.1, we derive truncation error bounds when the Laplace transform satisfies certain asymptotic conditions. It turns out that in many applications, these asymptotic conditions are satisfied and the involved parameters can be specified explicitly; see Sections 5–7. This then leads to computable truncation error bounds, based on which we can control the truncation error simply by choosing sufficiently large N_1 and N_2.

THEOREM 4.1. *For any fixed $\vec{t} \in \mathbb{R}^2$, $\vec{v} \in$ ROAC and $\vec{C} \geq 0$ such that $|t_j| + C_j > 0$ for $j = 1, 2$,*

(i) if there exist $\alpha_p > 1$ for $p = 1, \ldots, 4$, $\vec{M} \geq 0$, and positive functions $\zeta(\vec{v})$

and $\zeta_j(\vec{v},\omega_j)$ *for* $j=1,2$ *such that*

$$|L_f(\vec{v}+i\vec{\omega})| \le \begin{cases} \zeta_2(\vec{v},\omega_2)|\omega_1|^{-\alpha_1}, & \text{for all } \vec{\omega}\in D_1^{\vec{M}};\\ \zeta_1(\vec{v},\omega_1)|\omega_2|^{-\alpha_2}, & \text{for all } \vec{\omega}\in D_2^{\vec{M}};\\ \zeta(\vec{v})|\omega_1|^{-\alpha_3}|\omega_2|^{-\alpha_4}, & \text{for all } \vec{\omega}\in D_3^{\vec{M}}, \end{cases} \tag{13}$$

then the truncation error

$$|e_T(\vec{t},\vec{v},\vec{C},\vec{N})| \le \frac{e^{\vec{v}\cdot\vec{t}}}{2(|t_1|+C_1)(|t_2|+C_2)}\Big[B_1(\vec{N})+B_2(\vec{N})+B_3(\vec{N})\Big] \tag{14}$$

for any $\vec{N}\in\mathbb{N}^2$ *such that* $N_j > \frac{M_j}{b_j}-1$ *with* $b_j := |a_j| \equiv \frac{\pi}{|t_j|+C_j} > 0$ *for* $j=1,2$, *where*

$$\begin{aligned} B_1(\vec{N}) &= \frac{b_1^{-\alpha_1}}{\alpha_1-1}N_1^{1-\alpha_1}\sum_{k_2=-N_2}^{N_2}\zeta_2(\vec{v},k_2b_2sgn(t_2))\\ &= O\Big(N_1^{1-\alpha_1}\Big), \quad \text{for any fixed } N_2,\\ B_2(\vec{N}) &= \frac{b_2^{-\alpha_2}}{\alpha_2-1}N_2^{1-\alpha_2}\sum_{k_1=-N_1}^{N_1}\zeta_1(\vec{v},k_1b_1sgn(t_1))\\ &= O\Big(N_2^{1-\alpha_2}\Big), \quad \text{for any fixed } N_1,\\ B_3(\vec{N}) &= 2\zeta(\vec{v})\frac{b_1^{-\alpha_3}}{\alpha_3-1}\frac{b_2^{-\alpha_4}}{\alpha_4-1}N_1^{1-\alpha_3}N_2^{1-\alpha_4} = O\Big(N_1^{1-\alpha_3}N_2^{1-\alpha_4}\Big); \end{aligned}$$

(ii) if there exist $\rho_p>0$, $\xi_p>0$, $\alpha_p\in\mathbb{R}$ *for* $p=1,\dots,4$, $\vec{M}\ge 0$, *and positive-valued functions* $\zeta(\vec{v})$ *and* $\zeta_j(\vec{v},\omega_j)$ *for* $j=1,2$ *such that*

$$|L_f(\vec{v}+i\vec{\omega})| \le \begin{cases} \zeta_2(\vec{v},\omega_2)|\omega_1|^{-\alpha_1}e^{-\rho_1|\omega_1|^{\xi_1}}, & \text{for all } \vec{\omega}\in D_1^{\vec{M}};\\ \zeta_1(\vec{v},\omega_1)|\omega_2|^{-\alpha_2}e^{-\rho_2|\omega_2|^{\xi_2}}, & \text{for all } \vec{\omega}\in D_2^{\vec{M}};\\ \zeta(\vec{v})|\omega_1|^{-\alpha_3}|\omega_2|^{-\alpha_4}e^{-\rho_3|\omega_1|^{\xi_3}-\rho_4|\omega_2|^{\xi_4}}, & \text{for all } \vec{\omega}\in D_3^{\vec{M}}, \end{cases} \tag{15}$$

then the truncation error

$$|e_T(\vec{t},\vec{v},\vec{C},\vec{N})| \le \frac{e^{\vec{v}\cdot\vec{t}}}{2(|t_1|+C_1)(|t_2|+C_2)}\Big[B_1(\vec{N})+B_2(\vec{N})+B_3(\vec{N})\Big] \tag{16}$$

for any $\vec{N}\in\mathbb{N}^2$ *such that for* $j=1,2$,

$$N_j > \max\Big\{\frac{M_j}{b_j}, \frac{1}{b_j}\Big(\frac{\max\{-\alpha_j,0\}}{\xi_j\rho_j}\Big)^{\frac{1}{\xi_j}}, \frac{1}{b_{j+2}}\Big(\frac{\max\{-\alpha_{j+2},0\}}{\xi_{j+2}\rho_{j+2}}\Big)^{\frac{1}{\xi_{j+2}}}\Big\},$$

where

$$
\begin{aligned}
B_1(\vec{N}) &= \frac{\rho_1^{\frac{\alpha_1-1}{\xi_1}}}{b_1\xi_1}\Gamma\left(\frac{1-\alpha_1}{\xi_1}, \rho_1 b_1^{\xi_1} N_1^{\xi_1}\right) \sum_{k_2=-N_2}^{N_2} \zeta_2(\vec{v}, k_2 b_2 sgn(t_2)) \\
&= O\left(N_1^{1-\alpha_1-\xi_1} e^{-\rho_1 b_1^{\xi_1} N_1^{\xi_1}}\right), \quad \textit{for fixed } N_2, \\
B_2(\vec{N}) &= \frac{\rho_2^{\frac{\alpha_2-1}{\xi_2}}}{b_2\xi_2}\Gamma\left(\frac{1-\alpha_2}{\xi_2}, \rho_2 b_2^{\xi_2} N_2^{\xi_2}\right) \sum_{k_1=-N_1}^{N_1} \zeta_1(\vec{v}, k_1 b_1 sgn(t_1)) \\
&= O\left(N_2^{1-\alpha_2-\xi_2} e^{-\rho_2 b_2^{\xi_2} N_2^{\xi_2}}\right), \quad \textit{for fixed } N_1, \\
B_3(\vec{N}) &= 2\frac{\rho_3^{\frac{\alpha_3-1}{\xi_3}}}{b_1\xi_3}\frac{\rho_4^{\frac{\alpha_4-1}{\xi_4}}}{b_2\xi_4}\zeta(\vec{v})\Gamma\left(\frac{1-\alpha_3}{\xi_3}, \rho_3 b_1^{\xi_3} N_1^{\xi_3}\right)\Gamma\left(\frac{1-\alpha_4}{\xi_4}, \rho_4 b_2^{\xi_4} N_2^{\xi_4}\right)\Big\} \\
&= O\left(N_1^{1-\alpha_3-\xi_3} N_2^{1-\alpha_4-\xi_4} e^{-\rho_3 b_1^{\xi_3} N_1^{\xi_3} - \rho_4 b_2^{\xi_4} N_2^{\xi_4}}\right).
\end{aligned}
$$

Here, for any $s \in \mathbb{R}$ *and* $x > 0$, $\Gamma(s,x) := \int_x^{+\infty} y^{s-1}e^{-y}dy$. *When* $s > 0$, $\Gamma(s,x)$ *denotes the upper incomplete gamma function.*

PROOF. See Appendix C. □

Since in many cases, both discretization error bounds in Theorem 3.1 and truncation error bounds in Theorem 4.1 can be computed explicitly, we can control these two errors to achieve *any desired accuracy*, say 10^{-n} with $n \in \mathbb{N}$, by selecting the discretization parameter $\vec{C}$ and the truncation parameter $\vec{N}$ in the following two steps.

- **Step 1.** Based on Theorem 3.1, select sufficiently large $\vec{C} = (C_1, C_2)$ such that the discretization error is no greater than 0.5×10^{-n};
- **Step 2.** For fixed $\vec{C}$ chosen in Step 1, based on Theorem 4.1, select sufficiently large $\vec{N} = (N_1, N_2)$ such that the truncation error is no greater than 0.5×10^{-n}.

5. Application I: Spread options The spread option, whose payoff depends on the difference between two market variables, has been traded actively in various financial markets, including the equity derivatives market (index spread options), the commodity market (crack spread and crush spread options), and the energy market (spark spread options). However, no closed-form solutions are available for the spread option prices even under the BSM. But their two-dimensional Laplace transforms have explicit expressions under quite general models (Hurd and Zhou [17]). This section

TABLE 1

Connections among some Laplace transforms. Here $L_{Spr}(\vec{s})$ is derived based on Hurd and Zhou [17] and $B(x,y)$ denotes the beta function for x and y with $\Re(x)>0$ and $\Re(y)>0$

Original functions	Laplace transforms	ROACs
The joint pdf $f(\cdot)$	$L_f(\vec{s})$	ROAC of $L_f(\vec{s})$
The joint cdf $F(\cdot)$	$L_F(\vec{s}) = \frac{1}{s_1 s_2} L_f(\vec{s})$	$\mathbb{R}^2_+ \cap$ ROAC of $L_f(\vec{s})$
Spread option price $\mathrm{Spr}(\cdot)$	$L_{Spr}(\vec{s})$ $= e^{-rT} K \frac{B(-s_2, s_1+s_2-1)}{s_1(s_1-1)} L_f(-\vec{s})$	$\{\vec{v} : v_2 < 0, v_1 + v_2 > 1\} \cap$ ROAC of $L_f(-\vec{s})$

demonstrates that our two-dimensional, two-sided Laplace inversion algorithm can generate highly accurate numerical prices for spread options very fast as well as provide the related error bounds.

5.1. *Laplace transforms* The payoff function of the spread option is typically defined as $(S_1(T) - S_2(T) - K)^+$, where $K > 0$ is the strike price, T is the maturity, and

$$S_j(t) = e^{x_j(0) + X_j(t)} \qquad \text{for } j = 1, 2,$$

are prices of two correlated assets with respective return processes $\{X_j(t)\}$ and initial prices $e^{x_j(0)}$. Assume $ES_j(T) < +\infty$ for $j = 1, 2$, and that the two-dimensional, two-sided Laplace transform of the joint pdf $f(\vec{u})$ of $\vec{X}(T) := (X_1(T), X_2(T))$ for $\vec{u} \in \mathbb{R}^2$ is given by

$$\begin{aligned} L_f(\vec{s}) &:= \int_{-\infty}^{+\infty} \int_{-\infty}^{+\infty} e^{-\vec{s}\cdot\vec{u}} f(\vec{u}) du_1 du_2 \\ &\equiv E\left(e^{-\vec{s}\cdot\vec{X}(T)}\right), \quad \text{for any } \vec{v} := \Re(\vec{s}) \in \text{ROAC of } L_f. \end{aligned} \tag{17}$$

Then Table 1 provides the two-dimensional Laplace transform of its joint cdf as well as that of the following spread option price w.r.t. $\vec{u} := (x_1(0) - \log K, x_2(0) - \log K)$ under the given risk neutral measure $\mathbb{P}$

$$\begin{aligned} \mathrm{Spr}(\vec{u}) &:= e^{-rT} E\left[(S_1(T) - S_2(T) - K)^+\right] \\ &= e^{-rT} K E\left[\left(e^{u_1 + X_1(T)} - e^{u_2 + X_2(T)} - 1\right)^+\right]. \end{aligned} \tag{18}$$

The following proposition shows that under mild conditions our inversion formula (4) applies to evaluate the spread option prices and the joint cdf of the asset returns.

PROPOSITION 5.1. *(i) If $ES_j(T) < +\infty$ for $j = 1, 2$, $\vec{X}(T) \equiv (X_1(T), X_2(T))$ has a continuous distribution under the risk neutral measure $\mathbb{P}$, and*

TABLE 2
Specification of $\delta(\vec{y})$ for computing the discretization error bounds

	$\delta(\vec{y})$ in (8)
The joint cdf $F(\cdot)$	$\frac{1}{\pi^2 y_1 y_2} U(\vec{y})$
Spread option price $\mathrm{Spr}(\cdot)$	$\frac{e^{-rT} KB(-y_2, y_1+y_2-1)}{\pi^2 y_1(y_1-1)} U(-\vec{y})$

$\vec{0}$ belongs to the ROAC of $L_f(\vec{s})$, then both $F(\vec{u})$ and $Spr(\vec{u})$ satisfy Assumption 2.1;
(ii) If $L_f(\vec{s})$ satisfies either (13) except that $\alpha_p > 0, p = 1, \ldots, 4$, or (15), then $L_F(\vec{s})$ satisfies Assumption 2.2. If $L_f(-\vec{s})$ satisfies either (13) except that $\alpha_1 > -1$ and $\alpha_3 > -1$, or (15), then $L_{Spr}(\vec{s})$ satisfies Assumption 2.2.

PROOF. See Appendix D. □

5.2. *Discretization errors* To compute the discretization error bound in (9), it is required to specify the function $\delta(\vec{y})$ in (8) explicitly. As interpreted in Section 3.2.1, if for any fixed $\vec{y} \in \mathrm{ROAC}$, we can show $L_f(\vec{y} + i\vec{\omega})$ satisfies (13) or (15) and moreover, if we can find $L(\vec{y})$, $L_1(\vec{y})$ and $L_2(\vec{y})$ satisfying (11) (it is usually easy to find them because $L_f(\vec{y} + i\vec{\omega})$ is assumed to have a closed-form expression; see Section 5.4), then applying Proposition 3.2 and according to Table 1, we can specify respective $\delta(\vec{y})$ for $F(\cdot)$ and $\mathrm{Spr}(\cdot)$ immediately; see Table 2, where $U(\vec{y})$ is defined in (12).

5.3. *Truncation errors* To compute the truncation error bound in (14) or (16), we need to specify the parameters in (13) or (15). Indeed, if $L_f(\vec{s})$ satisfies (13) or (15) with known parameters, $L_F(\vec{s})$ and $L_{Spr}(\vec{s})$ also have similar asymptotic behaviors and related parameters can be easily obtained in Table 3. For instance, note that

$$\begin{aligned} |L_{Spr}(\vec{s})| &= e^{-rT} K \left| \frac{B(-s_2, s_1 + s_2 - 1)}{s_1(s_1 - 1)} L_f(-\vec{s}) \right| \\ &\le e^{-rT} KB(-v_2, v_1 + v_2 - 1) \frac{1}{|\omega_1|^2} |L_f(-\vec{s})| \end{aligned}$$

Hence, if $L_f(\vec{s})$ satisfies (13) with parameters M_1, M_2, α_1, α_2, α_3 and α_4, then $L_{Spr}(\vec{s})$ also satisfies (13) with parameters M_1, M_2, $\alpha_1 + 2$, α_2, $\alpha_3 + 2$ and α_4.

5.4. *Two examples* ***The BSM.*** Consider a two-dimensional BSM with risk-free interest rate r, volatilities σ_1, σ_2, dividends q_1, q_2, and correlation

TABLE 3
Connections among the parameters in (13) and (15) for computing the truncation error bounds. Here $j = 1, 2$ and $p = 1, \ldots, 4$

	Laplace transforms	Parameters in (13)	Parameters in (15)
The joint pdf $f(\cdot)$	$L_f(\vec{s})$	M_j, α_p	$M_j, \alpha_p, \rho_p, \xi_p$
The joint cdf $F(\cdot)$	$L_F(\vec{s})$	$M_j, \alpha_p + 1$	$M_j, \alpha_p + 1, \rho_p, \xi_p$
Spread option $\mathrm{Spr}(\cdot)$	$L_{Spr}(-\vec{s})$	$M_j, \alpha_p + 2 \times 1_{\{p \text{ is odd}\}}$	$M_j, \alpha_p + 2 \times 1_{\{p \text{ is odd}\}}$, ρ_p, ξ_p

$\rho \in (-1, 1)$. The asset returns $X_1(T)$ and $X_2(T)$ have a joint normal distribution and the Laplace transform of its joint pdf $f(\vec{u})$ is given by

$$L_f(\vec{s}) = \exp\left\{-s_1\left(r - q_1 - \frac{\sigma_1^2}{2}\right)T - s_2\left(r - q_2 - \frac{\sigma_2^2}{2}\right)T + \frac{(s_1^2\sigma_1^2 + s_2^2\sigma_2^2)T}{2} + s_1 s_2 \sigma_1 \sigma_2 \rho T\right\} \tag{19}$$

for $\Re(\vec{s}) \in \mathbb{R}^2$. Then the Laplace transforms of the joint cdf of $X_1(T)$ and $X_2(T)$ and the spread option price can be obtained immediately from Table 1. According to Proposition 5.1 and the following Proposition 5.2, our inversion formula (4) can be used to evaluate them by inverting their transforms.

The truncation error bounds related to the computation of the joint cdf and the spread option price can be derived by Theorem 4.1 with the parameters given in the following proposition.

PROPOSITION 5.2. *The two-sided Laplace transform $L_f(\vec{s})$ under the two-dimensional BSM satisfies (15) with the parameters $M_1 = M_2 = 0$, $\alpha_p = 0$, $\xi_p = 2$, $\rho_p = (1 - |\rho|)T/2$ for $p = 1, \ldots, 4$,*

$$\zeta(\vec{v}) = \exp\left\{T \times \left[-v_1\left(r - q_1 - \frac{\sigma_1^2}{2}\right) - v_2\left(r - q_2 - \frac{\sigma_2^2}{2}\right) + \frac{1}{2}v_1^2\sigma_1^2 + \frac{1}{2}v_2^2\sigma_2^2 + v_1 v_2 \sigma_1 \sigma_2 \rho\right]\right\}, \quad \textit{and}$$

$$\zeta_j(\vec{v}, \omega_j) = \zeta(\vec{v}) \exp\left\{-\frac{T(1 - |\rho|)}{2}\omega_j^2\right\}, \quad \textit{for } j = 1, 2.$$

The Laplace transforms $L_F(\vec{s})$ and $L_{Spr}(\vec{s})$ also satisfy (15) with the parameters given by Table 3.

PROOF. The proof follows immediately by noting that

$$|L_f(\vec{s})| = \zeta(\vec{v}) \exp\left\{(-T) \times \left(\frac{1}{2}\sigma_1^2\omega_1^2 + \frac{1}{2}\sigma_2^2\omega_2^2 + \omega_1\omega_2\sigma_1\sigma_2\rho\right)\right\}$$
$$\leq \zeta(\vec{v}) \exp\left\{-\frac{T(1-|\rho|)}{2}(\vec{\omega}\cdot\vec{\omega})\right\}. \qquad \square$$

The discretization error bounds related to the computation of the joint cdf and the spread option price can be obtained by Theorem 3.1 and Table 2, where $U(\vec{y}) = \frac{\pi}{2T(1-|\rho|)}\zeta(\vec{y})$ can be found easily because $M_1 = M_2 = 0$.

The Variance Gamma (VG) Model. Under the two-dimensional VG Model, the Laplace transform of the joint pdf $f(\vec{u})$ of the asset returns $X_1(T)$ and $X_2(T)$ has the following closed-form expression (see [17])

$$L_f(\vec{s}) = \left[1 - \left(\frac{1}{a_-} - \frac{1}{a_+}\right)(s_1+s_2) - \frac{(s_1+s_2)^2}{a_-a_+}\right]^{-\alpha\lambda T} \times \prod_{j=1}^{2}\left[1 - \left(\frac{1}{a_-} - \frac{1}{a_+}\right)s_j - \frac{s_j^2}{a_-a_+}\right]^{-(1-\alpha)\lambda T} \tag{20}$$

for $\vec{v} \equiv \Re(\vec{s}) \in \{\vec{v} \in \mathbb{R}^2 : v_j \in (-a_+, a_-), j = 1,2, \text{ and } v_1 + v_2 \in (-a_+, a_-)\}$, where $0 < \alpha < 1$, $a_- > 0$, $a_+ > 1$ and $\lambda > 0$.

Like the BSM, from Table 1 we can obtain the Laplace transforms of the joint cdf of $X_1(T)$ and $X_2(T)$ and the spread option price immediately. Proposition 5.1 and the following Proposition 5.3 indicate that our inversion formula (4) can be applied to evaluate them by inverting their transforms. Furthermore, the truncation error bounds for the joint cdf of $X_1(T)$ and $X_2(T)$ and the spread option price can also be derived by Theorem 4.1 with the parameters given in Proposition 5.3.

PROPOSITION 5.3. *The two-sided Laplace transform $L_f(\vec{s})$ under the two-dimensional VG model satisfies (13) with the parameters $\alpha_p = 2(1-\alpha)\lambda T$ for $p = 1, \ldots, 4$, $M_j = \max\{a_+ + v_j, a_- - v_j\}$ for $j = 1, 2$,*

(21)

$$\zeta(\vec{v}) = (a_-a_+)^{2(1-\alpha)\lambda T}\left[1 - \left(\frac{1}{a_-} - \frac{1}{a_+}\right)(v_1+v_2) - \frac{(v_1+v_2)^2}{a_-a_+}\right]^{-\alpha\lambda T}, \text{ and}$$

$$\zeta_j(\vec{v}, \omega_j) = \zeta(\vec{v})\left(\max\left\{(a_- - v_j)\cdot(a_+ + v_j), |\omega_j|^2\right\}\right)^{-(1-\alpha)\lambda T}, \text{ for } j = 1, 2.$$

The Laplace transforms $L_F(\vec{s})$ and $L_{Spr}(\vec{s})$ also satisfy (13) with the parameters given by Table 3.

PROOF. See Appendix D. □

Besides, the discretization error bounds for the joint cdf and the spread option price can be obtained by Theorem 3.1 and Table 2, where we can simply select $L(\vec{y}) = L_f(\vec{y})$, $L_1(\vec{y}) = |L_f(y_1, y_2+iM_2)|$, and $L_2(\vec{y}) = |L_f(y_1+iM_1, y_2)|$.

6. Application II: Barrier options The pricing of barrier options relies heavily upon the joint distribution of the terminal asset return and the first passage time. Accordingly, analytical solutions are usually unavailable under general asset pricing models. Under the double-exponential jump diffusion model (DEM, see Kou [18]), Kou et al. [20] derived a closed-form two-dimensional Laplace transform for the barrier option price w.r.t. the transformed strike and the maturity. This section will apply our inversion formula (4) to compute the barrier option price and the joint cdf of the terminal asset return and the first passage time under the DEM. The computable bounds for both the discretization and truncation errors will also be provided.

6.1. *Laplace transforms* In the DEM, the asset price S_t under the risk neutral measure $\mathbb{P}$ is given by

$$S_t = S_0 e^{X_t} \quad \text{with the asset return} \quad X_t = \mu t + \sigma W_t + \sum_{i=1}^{N_t} Y_i,$$

where $\mu = r - \frac{\sigma^2}{2} - \lambda\zeta$, $\zeta = \frac{p\eta}{\eta-1} + \frac{q\theta}{\theta+1} - 1$, r is the risk free interest rate, σ is the volatility, $\{W_t : t \geq 0\}$ is a standard Brownian motion, $\{N_t : t \geq 0\}$ is a Poisson process with rate λ, and $\{Y_i : i = 1, 2, \ldots\}$ are independent and identically distributed double exponential random variables with the pdf

(22)
$$f_Y(x) = p\eta e^{-\eta x} 1_{\{x\geq 0\}} + q\theta e^{\theta x} 1_{\{x<0\}}, \quad \text{with } \eta > 1,\ p+q = 1,\ p,\ q,\ \theta \in \mathbb{R}^+.$$

The Lévy exponent of this double exponential jump diffusion process X_t is

$$G(z) := \frac{\log E e^{zX_t}}{t} = \frac{\sigma^2 z^2}{2} + \mu z + \lambda\left(\frac{p\eta}{\eta - z} + \frac{q\theta}{\theta + z} - 1\right), \text{ for } \Re(z) \in (-\theta, \eta). \tag{23}$$

Denote the first passage time of $\{X_t : t \geq 0\}$ to a flat barrier b by:

$$\tau_b := \inf\{t : X_t \geq b\},$$

TABLE 4
Connection among several transforms related to barrier options under the DEM

Original functions	Laplace transforms	ROACs
The joint pdf $f_{\tau_b, X_{\tau_b}}(\cdot)$	$L_f(\vec{s})$	ROAC of $L_f(\vec{s})$
The joint cdf $F_{\tau_b, X_T}(\cdot)$	$L_F(\vec{s}) = \frac{L_f(s_1,-s_2)}{s_2(s_1-G(s_2))}$	$\{\vec{v} : 0 < v_2 < \eta, v_1 > \max\{G(v_2), 0\}\}$ $\cap$ ROAC of $L_f(s_1, -s_2)$
UIC barrier option UIC$(\cdot)$	$L_{\text{UIC}}(\vec{s}) = \frac{S_0^{s_2+1} L_f(s_1+r,-s_2-1)}{s_2(s_2+1)(s_1+r-G(s_2+1))}$	$\{\vec{v} : 0 < v_2 < \eta - 1, v_1 > (G(v_2+1) - r)^+\}$ $\cap$ ROAC of $L_f(s_1 + r, -s_2 - 1)$

where $b > 0$ and $X_{\tau_b} := \limsup_{t\to+\infty} X_t$ on the set $\{\tau_b = +\infty\}$. Kou and Wang [19] derived the Laplace transform of the joint pdf $f_{\tau_b, X_{\tau_b}}$ of τ_b and X_{τ_b}:

$$L_f(\vec{s}) = \frac{\eta - \beta_{1,s_1}}{\beta_{2,s_1} - \beta_{1,s_1}} e^{-bs_2 - b\beta_{1,s_1}} \left(1 + \frac{\beta_{2,s_1} - \eta}{\eta + s_2}\right) + \frac{\beta_{2,s_1} - \eta}{\beta_{2,s_1} - \beta_{1,s_1}} e^{-bs_2 - b\beta_{2,s_1}} \left(1 + \frac{\beta_{1,s_1} - \eta}{\eta + s_2}\right), \tag{24}$$

for $\Re(\vec{s}) \in (0, +\infty) \times (-\eta, +\infty)$, where β_{1,s_1} and β_{2,s_1} are the two roots of the equation $G(z) = s_1$ with positive real parts.

Consider an up-and-in call (UIC) barrier option with the barrier $H > S_0$, the strike K, and the maturity T. Its price under the risk neutral measure $\mathbb{P}$ is given by

$$\text{UIC}(T, k) = e^{-rT} E\left[(S_0 e^{X_T} - e^{-k})^+ 1_{\{\tau_b < T\}}\right],$$

where $k := -\log K$ and $b := \log(H/S_0) > 0$. Besides, we are interested in the joint cdf of τ_b and X_T, or equivalently the following probability

$$F_{\tau_b, X_T}(\vec{t}) := P(\tau_b \le t_1, X_T \ge -t_2).$$

Kou et al. [20] derived closed-form two-dimensional Laplace transforms of the joint cdf $F_{\tau_b, X_T}(\vec{t})$ w.r.t. t_1 and t_2 as well as that of the UIC barrier option price UIC(T, k) w.r.t. T and k; see Table 4. We point out that it is not easy to determine the ROAC of $L_f(\vec{s})$. Kou and Wang [19] showed $(0, +\infty) \times (-\eta, +\infty) \subset$ ROAC of $L_f(\vec{s})$, whereas Cai and Sun [8] proved that $L_f(\vec{s})$ exists for a larger set, i.e., for $\Re(\vec{s}) \in [\mathbb{M}(G), +\infty) \times (-\eta, +\infty)$, where $\mathbb{M}(G) := \min_{x\in(-\theta,\eta)} G(x)$.

The following proposition shows that our inversion formula (4) is applicable to the evaluation of the joint cdf $F_{\tau_b, X_T}(\cdot)$ and the UIC barrier option price UIC$(\cdot)$.

PROPOSITION 6.1. *Under the DEM, we have (i) both $F_{\tau_b,X_T}(\cdot)$ and UIC$(\cdot)$ satisfy Assumption 2.1, and (ii) both $L_F(\vec{s})$ and $L_{UIC}(\vec{s})$ satisfy Assumption 2.2.*

PROOF. See Appendix F. □

6.2. *Discretization errors* To compute the discretization error bounds in (9) via Theorem 3.1, we are required to specify the function $\delta(\vec{y})$ in (8). To this end, we can still apply Proposition 3.2 and the method in Section 3.2.1 by using the result in the following Proposition 6.2 in Section 6.3. Here we provide a more straightforward approach alternatively. For any $\vec{v}$ in the respective ROACs,

$$\begin{aligned} e^{-\vec{v}\cdot\vec{t}}|F_{\tau_b,X_T}(t_1,t_2)| &\le e^{-\vec{v}\cdot\vec{t}}P(X_2 \ge -t_2) \le e^{-\vec{v}\cdot\vec{t}}Ee^{v_2(X_2+t_2)} \\ &\le Ee^{v_2X_2} = e^{G(v_2)T}; \\ e^{-v_1T-v_2k}|\mathrm{UIC}(T,k)| &\le e^{-(v_1+r)T-v_2k}E\left[S_0e^{X_T}1_{\{X_T+\log S_0+k\ge 0\}}\right] \\ &\le e^{-(v_1+r)T-v_2k}E\left[S_0e^{X_T}e^{v_2(X_T+\log S_0+k)}\right] \\ &= S_0^{v_2+1}e^{G(v_2+1)T-(v_1+r)T} \le S_0^{v_2+1}. \end{aligned}$$

Consequently, we can simply select $\delta(\vec{y}) = e^{G(y_2)T}$ for $F_{\tau_b,X_T}(\cdot)$ and $\delta(\vec{y}) = S_0^{v_2+1}$ for UIC$(\cdot)$.

6.3. *Truncation errors* To calculate the truncation error bounds via Theorem 4.1, we need to specify the asymptotic behavior of $L_F(\vec{s})$ and $L_{\mathrm{UIC}}(\vec{s})$. The following proposition shows both of them satisfy (13) with explicit parameters.

PROPOSITION 6.2. *(i) For any $\vec{v} \in$ ROAC of $L_F(\vec{s})$, the function $L_F(\vec{s})$ satisfies (10) with $\alpha_1 = 2$, $\alpha_2 = 3$, $\alpha_3 = \frac{3}{2}$, $\alpha_4 = 2$, and other associated parameters explicitly specified in (44).*
(ii) For any $\vec{v} \in$ ROAC of $L_{UIC}(\vec{s})$, the function $L_{UIC}(\vec{s})$ satisfies (10) with $\alpha_1 = 2$, $\alpha_2 = 4$, $\alpha_3 = \frac{3}{2}$, $\alpha_4 = 3$, and other associated parameters explicitly specified in (45).

PROOF. See Appendix G. □

7. Application III: Computing sensitivities In Sections 5 and 6, we apply our inversion formula to evaluate certain joint cdfs and exotic option prices. This section will illustrate that it can also be used to compute sensitivities or greeks of options.

TABLE 5
Laplace transforms of two deltas $\Delta_1(\vec{u})$ and $\Delta_2(\vec{u})$ of the spread option

Functions	Laplace transforms	ROACs
$\Delta_1(\vec{u})$	$L_{\Delta_1}(\vec{s}) = e^{-rT}K\frac{B(-s_2,s_1+s_2)}{s_1}$ $\times L_f(-1-s_1,-s_2)$	$\{\vec{v}: v_2<0, v_1+v_2>0\}\cap$ ROAC of $L_f(-1-s_1,-s_2)$
$\Delta_2(\vec{u})$	$L_{\Delta_2}(\vec{s}) = e^{-rT}K\frac{(s_2+1)B(-1-s_2,s_1+s_2)}{s_1(s_1-1)}$ $\times L_f(-s_1,-1-s_2)$	$\{\vec{v}: v_2<-1, v_1+v_2>0\}\cap$ ROAC of $L_f(-s_1,-1-s_2)$

We take two deltas of spread options as an example and use the same notations as in Section 5. Assume $L_f(\vec{s})$ is the two-dimensional Laplace transform of the joint pdf of two underlying asset returns $X_1(T)$ and $X_2(T)$; see (17). Then the Laplace transform $L_{\text{Spr}}(\vec{s})$ of the spread option price w.r.t. $\vec{u} \equiv (X_1(0) - \log K, X_2(0) - \log K)$ is given by (see Table 1)

$$L_{\text{Spr}}(\vec{s}) = e^{-rT}K\frac{B(-s_2, s_1+s_2-1)}{s_1(s_1-1)}L_f(-\vec{s}), \tag{25}$$

for $\vec{v} \equiv \Re(\vec{s}) \in \{v_2 < 0, v_1 + v_2 > 0\}\cap$ ROAC of $L_f(\vec{s})$. Consider two deltas of spread options as follows.

$$\Delta_1(\vec{u}) := \frac{\partial \text{Spr}(\vec{u})}{\partial S_1(0)} \quad \text{and} \quad \Delta_2(\vec{u}) := \frac{\partial \text{Spr}(\vec{u})}{\partial S_2(0)}$$

Differentiating (25) w.r.t. $S_1(0)$ and $S_2(0)$ respectively and interchanging derivatives and integrals based on Theorem A.12 in Schiff [25] yields Laplace transforms of the two deltas; see Table 5.

Under similar mild conditions as in Proposition 5.1, we can show that our inversion algorithm is valid for computing $\Delta_1(\vec{u})$ and $\Delta_2(\vec{u})$.

PROPOSITION 7.1. *(i) If $ES_j(T) < +\infty$ for $j = 1, 2$, $\vec{X}(T) \equiv (X_1(T), X_2(T))$ has a continuous distribution under the risk neutral measure $\mathbb{P}$, and $\vec{0}$ belongs to the ROAC of $L_f(\vec{s})$, then both of the functions $\Delta_1(\vec{u})$ and $\Delta_2(\vec{u})$ satisfy Assumption 2.1.*
(ii) If $L_f(-1-s_1,-s_2)$ satisfies (13) except $\alpha_1 > 0$ and $\alpha_3 > 0$, or satisfies (15), then $L_{\Delta_1}(\vec{s})$ satisfies Assumption 2.2; if $L_f(-s_1,-1-s_2)$ satisfies (13) except $\alpha_1 > 0$, $\alpha_2 > 2$, $\alpha_3 > 0$ and $\alpha_4 > 2$, or satisfies (15), then $L_{\Delta_2}(\vec{s})$ satisfies Assumption 2.2.

PROOF. The argument of (ii) is straightforward by Table 7, and (i) can be shown in the same way as for Proposition 5.1. □

7.1. *Discretization errors* To compute discretization error bounds via Theorem 3.1, we derive the required functions $\delta(\vec{y})$ in (8) in a similar manner as in Section 5.2; see Table 6.

TABLE 6
Specification of $\delta(\vec{y})$ for computing discretization error bounds of two deltas. Here $U(\vec{y})$ is defined in (12)

	$\delta(\vec{y})$ in (8)
$\Delta_1(\vec{u})$	$\frac{e^{-rT}KB(-y_2,y_1+y_2)}{\pi^2 y_1}U(-1-y_1,-y_2)$
$\Delta_2(\vec{u}))$	$\frac{e^{-rT}K\cdot\lvert y_2+1+iM_2\rvert\cdot B(-y_2-1,y_1+y_2)}{\pi^2 y_1(y_1-1)}U(-y_1,-1-y_2)$

TABLE 7
Connections among the parameters in (13) and (15) for computing the truncation error bounds of two deltas. Here $j=1,2$ and $p=1,\ldots,4$. Without loss of generality, we assume $M_2 \geq |v_2|+1$ here

	Laplace transforms	Parameters in (13)	Parameters in (15)
The pdf $f(\cdot)$	$L_f(\vec{s})$	M_j, α_p	$M_j, \alpha_p, \rho_p, \xi_p$
$\Delta_1(\vec{u})$	$L_{\Delta_1}(-1-s_1,-s_2)$	$M_j, \alpha_p + 1_{\{p \text{ is odd}\}}$	$M_j, \alpha_p + 1_{\{p \text{ is odd}\}}$, ρ_p, ξ_p
$\Delta_2(\vec{u})$	$L_{\Delta_2}(-s_1,-1-s_2)$	M_j, $\alpha_p - 1 + 3\times 1_{\{p \text{ is odd}\}}$	$M_j, \alpha_p - 1 + 3\times 1_{\{p \text{ is odd}\}}$, ρ_p, ξ_p

7.2. *Truncation errors* To calculate truncation error bounds via Theorem 4.1, we need to specify the asymptotic behavior of $L_{\Delta_1}(\vec{s})$ and $L_{\Delta_2}(\vec{s})$. According to their explicit expressions, we obtain

$$|L_{\Delta_1}(\vec{s})| \leq e^{-rT}KB(-v_2, v_1+v_2)\frac{1}{|\omega_1|}|L_f(-1-s_1,-s_2)|,$$
$$|L_{\Delta_2}(\vec{s})| \leq e^{-rT}KB(-v_2-1, v_1+v_2)\frac{\sqrt{2}|\omega_2|}{|\omega_1|^2}|L_f(-s_1,-1-s_2)|,$$

for $|\omega_2| \geq |v_2|+1$. Consequently, if the asymptotic behavior of $L_f(\vec{s})$ satisfies (13) or (15) with explicit parameters, then $L_{\Delta_1}(\vec{s})$ and $L_{\Delta_2}(\vec{s})$ also satisfy (13) or (15) with parameters given in Table 7.

8. Numerical examples In this section we provide numerical results for the quantities of interest discussed in Sections 5–7, by inverting their respective two-dimensional Laplace transforms via our inversion formula (4). The numerical results indicate that our algorithm is very accurate and fast. The major difference from most of other numerical methods is that our algorithm also generates discretization and truncation error bounds, which tell us how accurate the numerical results are. Indeed, we can control these two errors to any desired accuracy by selecting sufficiently large parameters $\vec{C}$ and $\vec{N}$. Therefore, our algorithm is especially suitable to provide benchmarks. All numerical experiments here are conducted via MATLAB R2011a on a desktop computer with 2.85GB of RAM and an Intel Core i5-2500

TABLE 8

Pricing spread call options and evaluating the joint cdf $P(X_1(T) \le x_1, X_2(T) \le x_2)$ under the two-dimensional BSM. The column "Cai & Shi" denotes numerical results obtained via our algorithm. The column "Hurd & Zhou" is taken from Table 1 of [17]. "True values" are calculated from the analytical formula of the joint normal cdf. The model parameters are the same as in Table 1 of [17], i.e., $r = 0.1$, $\sigma_1 = 0.2$, $\sigma_2 = 0.1$, $q_1 = q_2 = 0.05$, $S_1(0) = 100$, $S_2(0) = 96$, $\rho = 0.5$ and $T = 1$. The inversion algorithm parameters are $v_1 = 7$, $v_2 = -2$, $C_1 = C_2 = 10$, $N_1 = 400$ and $N_2 = 600$ for the top panel, and $x_2 = 0.1$, $v_1 = v_2 = 3$, $C_1 = C_2 = 7$ and $N_1 = N_2 = 200$ for the bottom panel. It takes around 1 second and 0.03 seconds to generate one numerical result for the spread option price and the joint cdf, respectively, via our algorithm

Pricing spread call options under the two-dimensional BSM

K	Cai & Shi	UB of disc. err.	UB of trunc. err.	Hurd & Zhou	Abs. err.
0.4	8.31246073	3.2E-9	6.3E-9	8.312461	0.000000
0.8	8.11499376	9.4E-11	5.3E-12	8.114994	0.000000
1.2	7.92081978	1.2E-11	6.7E-14	7.920820	0.000000
1.6	7.72993249	2.7E-12	2.7E-15	7.729932	0.000000
2.0	7.54232390	8.7E-13	2.0E-16	7.542324	0.000000
2.4	7.35798430	3.5E-13	2.3E-17	7.357984	0.000000
2.8	7.17690236	1.6E-13	3.6E-18	7.176902	0.000000
3.2	6.99906512	8.0E-14	6.9E-19	6.999065	0.000000
3.6	6.82445805	4.4E-14	1.6E-19	6.824458	0.000000
4.0	6.65306511	2.6E-14	4.1E-20	6.653065	0.000000

Evaluating the joint cdf $P(X_1(T) \le x_1, X_2(T) \le x_2)$ under the two-dimensional BSM

x_1	Cai & Shi	UB of disc. err.	UB of trunc. err.	True values	Abs. err.
-1	0.0000001302	1.2E-11	1.6E-12	0.0000001302	0.0000000000
-0.5	0.0039833228	4.1E-12	7.1E-12	0.0039833228	0.0000000000
-0.3	0.0476656931	3.0E-12	1.3E-11	0.0476656931	0.0000000000
-0.1	0.2333029204	2.4E-12	2.4E-11	0.2333029204	0.0000000000
0	0.3801785475	1.7E-12	3.2E-11	0.3801785475	0.0000000000
0.1	0.5212051305	1.5E-12	4.3E-11	0.5212051305	0.0000000000
0.3	0.6782910666	1.3E-12	7.8E-11	0.6782910666	0.0000000000
0.5	0.7071168688	1.3E-12	1.4E-10	0.7071168688	0.0000000000

(3.3GHz) processor. The codes are available on the first author's website http://ihome.ust.hk/~ningcai/index_IELM_1.html.

8.1. *Evaluating spread options and related joint CDF in the BSM and VG* Table 8 gives numerical results (denoted by "Cai & Shi") for the spread call options and the joint cdf of the asset returns under the two-dimensional BSM via our inversion formula (4) as well as the related discretization and truncation error bounds. We can see that our algorithm is highly accurate and efficient. (i) Our numerical results for the spread option prices agree

with those obtained by Hurd and Zhou [17] (denoted by "Hurd & Zhou") to 6 decimal points. In fact, our algorithm is much more accurate than reflected from the comparison with Hurd and Zhou [17] because the error bounds indicate that our results have achieved the accuracy of $10^{-9} \sim 10^{-14}$. (ii) Our numerical results for the joint cdf agree with the true values to 10 decimal points. Besides, our algorithm is robust because even in the extreme case $x_1 = -1$ where the probability is very small, our algorithm is still highly accurate with reliable error bounds. (iii) It takes only 1 second and 0.03 seconds to generate one numerical result for the spread option price and the joint cdf, respectively, via our algorithm.

Similarly, Table 9 provides numerical results for the spread call option prices and the joint cdf of the asset returns under the two-dimensional VG model as well as the associated error bounds. It is indicated that our algorithm is still highly accurate and efficient.

8.1.1. *Pricing spread options in the "deep out of the money" case* As pointed out by Carr and Madan [10], the plain FFT might break down for deep out of the money European call options and even generate negative values. In this section, we intend to apply our two-dimensional, two-sided Laplace inversion method to price the spread call options in a similar "deep out of the money" case, where $S_2(0) + K$ is much larger than $S_1(0)$. Specifically, under both the two-dimensional BSM and the VG model, we set $S_1(0) = 100$ and let $S_2(0) + K$ vary from 120 to 200 with increment 10. The numerical spread option prices are given in Table 10. We can see that our algorithm is still highly accurate even in the extreme cases, e.g., $S_2(0) + K = 180$, 190 and 200. This implies that our algorithm is quite robust.

8.1.2. *The special case $K = 0$ under the BSM* When $K = 0$, the spread option price under the two-dimensional BSM has an analytical formula; see (29) in Appendix E. Furthermore, its Laplace transform also becomes simpler in this special case. In fact, its single Laplace transform w.r.t. $X_2(0)$ has a closed-form expression given by (30) in Appendix E. Then the one-dimensional, two-sided Euler inversion algorithm applies as a special case of our two-dimensional algorithm. Moreover, the related discretization and truncation error bounds can be derived similarly. See Appendix E for more details. Table 11 reports the comparison between our Laplace inversion results and the true values obtained from the analytical formula, and also provides the associated discretization and truncation error bounds. It can be seen that the inversion method is still highly accurate.

TABLE 9

Pricing spread call options and evaluating the joint cdf $P(X_1(T) \le x_1, X_2(T) \le x_2)$ under the two-dimensional VG model. The column "Cai & Shi" denotes numerical results obtained via our algorithm. The column "Hurd & Zhou" is taken from Table 3 of [17]. "MC values" and "Std. err." are Monte Carlo simulation estimates and associated standard errors, respectively, obtained using a sample size of 10^7. The model parameters are the same as n Table 3 of [17], i.e., $r = 0.1$, $a_- = 24.4499$, $a_+ = 20.4499$, $\alpha = 0.4$, $\lambda = 10$, $S_1(0) = 100$, $S_2(0) = 96$, $\rho = 0.5$, and $T = 1$. The inversion algorithm parameters are $v_1 = 7$, $v_2 = -2$, $C_1 = 7$, $C_2 = 6$, $N_1 = 300$ and $N_2 = 600$ for the top panel, and $x_2 = 0.1$, $v_1 = v_2 = 3$, $C_1 = C_2 = 7$ and $N_1 = N_2 = 200$ for the bottom panel. It takes around 0.8 second and 0.05 seconds to generate one numerical result for the spread option price and the joint cdf, respectively, via our algorithm

Pricing spread call options under the two-dimensional VG model

K	Cai & Shi	UB of disc. err.	UB of trunc. err.	Hurd & Zhou	Abs. err.
2.0	9.727458	6.7E-6	2.2E-5	9.727458	0.000000
2.2	9.630006	4.1E-6	1.2E-5	9.630005	0.000001
2.4	9.533200	2.6E-6	7.1E-6	9.533199	0.000001
2.6	9.437040	1.8E-6	4.3E-6	9.437040	0.000000
2.8	9.341528	1.2E-6	2.7E-6	9.341527	0.000001
3.0	9.246662	8.5E-7	1.8E-6	9.246662	0.000000
3.2	9.152445	6.1E-7	1.2E-6	9.152445	0.000000
3.4	9.058875	4.5E-7	8.2E-7	9.058875	0.000000
3.6	8.965954	3.3E-7	5.7E-7	8.965954	0.000000
3.8	8.873681	2.5E-7	4.1E-7	8.873681	0.000000
4.0	8.782057	2.0E-7	3.0E-7	8.782057	0.000000

Evaluating the joint cdf $P(X_1(T) \le x_1, X_2(T) \le x_2)$ under the two-dimensional VG model

x_1	Cai & Shi	UB of disc. err.	UB of trunc. err.	MC values (Std. err.)	Abs. err.
−1	0.00000075	2.9E-9	2.6E-11	0.00000050 (0.00000022)	0.00000025
−0.5	0.00203320	1.1E-9	6.6E-11	0.00200914 (0.00001405)	0.00002406
−0.3	0.02349541	7.8E-10	9.8E-11	0.02355573 (0.00004540)	−0.00006032
−0.1	0.13879889	6.6E-10	1.5E-10	0.13881740 (0.00008944)	−0.00001851
0	0.24898022	6.6E-10	1.9E-10	0.24894320 (0.00010146)	0.00003702
0.1	0.36606506	4.8E-10	2.7E-10	0.36614173 (0.00010571)	−0.00007667
0.3	0.51059581	4.5E-10	5.9E-10	0.51067527 (0.00011211)	−0.00007946
0.5	0.54472360	4.5E-10	1.3E-9	0.54478029 (0.00011704)	−0.00005669

TABLE 10

Pricing spread options under the two-dimensional BSM and VG model in the "deep out of the money" case. The column "Cai & Shi" denotes numerical results obtained via our algorithm, while "MC values" and "Std. err." are Monte Carlo estimates and associated standard errors, respectively, obtained by simulating 10^7 *samples. All the model parameters are the same as in Table 8 for the BSM and in Table 9 for the VG model. The parameters for the inversion algorithm are* $v_1 = 7$, $v_2 = -2$, $C_1 = C_2 = 10$, $N_1 = 400$ *and* $N_2 = 600$ *for the BSM, and* $v_1 = 7$, $v_2 = -2$, $C_1 = 7$, $C_2 = 6$, $N_1 = 300$ *and* $N_2 = 600$ *for the VG model. It takes around 1 second and 0.6 seconds to produce one numerical result under the BSM and the VG model, respectively*

Pricing spread call options under the two-dimensional BSM in the "deep out of the money" case

$S_2(0) + K$	Cai & Shi	UB of disc. err.	UB of trunc. err.	MC values	Std. err.	Abs. err.
120	1.53065155	1.2E-17	1.3E-31	1.529657	0.001410	0.000997
130	0.65133480	6.6E-18	2.7E-34	0.650397	0.001000	0.000937
140	0.26157215	4.6E-18	2.2E-36	0.261200	0.000660	0.000372
150	0.10052638	3.8E-18	3.9E-38	0.100450	0.000416	0.000076
160	0.03739572	3.6E-18	1.2E-39	0.037423	0.000256	−0.000027
170	0.01358880	3.9E-18	5.5E-41	0.013667	0.000155	−0.000078
180	0.00485842	4.7E-18	3.4E-42	0.004915	0.000093	−0.000057
190	0.00171883	6.4E-18	2.7E-43	0.001748	0.000056	−0.000029
200	0.00060442	5.4E-18	4.7E-43	0.000620	0.000034	−0.000016

Pricing spread call options under the two-dimensional VG model in the "deep out of the money" case

$S_2(0) + K$	Cai & Shi	UB of disc. err.	UB of trunc. err.	MC values	Std. err.	Abs. err.
120	2.66155555	4.1E-11	3.3E-12	2.657996	0.001964	0.003560
130	1.34263221	2.2E-11	3.4E-13	1.340673	0.001558	0.001959
140	0.65757636	2.8E-11	6.1E-14	0.656471	0.001172	0.001105
150	0.31851544	4.9E-11	1.6E-14	0.317920	0.000856	0.000595
160	0.15464860	8.9E-11	5.0E-15	0.154085	0.000617	0.000664
170	0.07592838	1.6E-10	1.9E-15	0.075502	0.000445	0.000426
180	0.03789519	2.7E-10	7.9E-16	0.037695	0.000322	0.000200
190	0.01928059	4.4E-10	3.7E-16	0.019220	0.000235	0.000061
200	0.01001325	4.2E-10	2.3E-16	0.010033	0.000174	−0.000020

8.2. *Evaluating barrier options and related joint CDF under the DEM* In Table 12, we provide numerical results for the up-and-in call barrier option prices and the quantity $P(\tau_b \le x_1, X_T \ge -x_2)$ under the DEM as well as the related error bounds. Note that in this case, the truncation error is not as easy to control as for the spread options. This is primarily because the truncation error bounds decay more slowly in a power way; see Propo-

TABLE 11

Pricing spread options when $K = 0$ under the two-dimensional BSM. The column "Cai & Shi" denotes numerical results obtained via Laplace inversion algorithm, while "True values" are computed from the analytical formula (29). The model parameters are the same as in Table 8 except that $S_2(0)$ varies from 80 to 120. The inversion algorithm parameters are $v = -2$, $C = 2$, and $N = 80$. It takes approximately 0.0003 seconds to generate one spread option price via our algorithm

Pricing spread options under the two-dimensional BSM when $K = 0$					
$S_2(0)$	Cai & Shi	UB of disc. err.	UB of trunc. err.	True values	Abs. err.
80	19.710565	4.8E-7	6.4E-9	19.710565	0.000000
85	15.686513	3.8E-7	8.6E-9	15.686513	0.000000
90	12.108034	3.0E-7	1.1E-8	12.108034	0.000000
95	9.056493	2.4E-7	1.4E-8	9.056493	0.000000
100	6.564677	2.0E-7	1.8E-8	6.564677	0.000000
105	4.615204	1.6E-7	2.2E-8	4.615204	0.000000
110	3.151297	1.4E-7	2.7E-8	3.151297	0.000000
115	2.093444	1.1E-7	3.2E-8	2.093444	0.000000
120	1.355646	9.7E-8	3.7E-8	1.355646	0.000000

sition 6.2. However, the numerical results are still accurate compared with the benchmarks.

8.3. *Computing two deltas of spread options in the BSM and VG model* Table 13 gives numerical results for two deltas of spread options under the BSM and VG model as well as the related error bounds. It can be seen that all the numerical results stay within the 95% confidence intervals of the associated Monte Carlo simulation estimates. Indeed, the error bounds indicate that the numerical results are more accurate than reflected from the comparison with the Monte Carlo estimates. Besides, the algorithm is very efficient in that it takes only 0.7 seconds to generate one numerical result.

9. Conclusions This paper is devoted to the development of a two-dimensional, two-sided Euler inversion algorithm with computable bounds for both discretization and truncation errors. This algorithm is especially useful to provide benchmarks in that the computable error bounds make it possible for us to select the algorithm parameters properly to achieve any desired accuracy. Since the error bounds decay quickly, e.g., exponentially, in many cases, the algorithm is very efficient. Numerical experiments of applying this algorithm to the valuation of some exotic options and joint cdfs suggest that the algorithm is accurate, fast, and simple to implement.

Z-transforms can be considered as the counterpart of Laplace transforms in the discrete case and also have many applications in operations research

TABLE 12

Pricing up-and-in call barrier options and evaluating $P(\tau_b \le x_1, X_T \ge -x_2)$ under the DEM. The column "Cai & Shi" denotes numerical results obtained via our algorithm. The column "KPW" is taken from Table 4 of Kou et al. [20]. "MC values" and "Std. err." are Monte Carlo simulation estimates and associated standard errors, respectively, obtained by simulating $50,000$ samples and using $20,000$ time steps. The model parameters are the same as in [20], i.e., $S_0 = 100$, $H = 115$, $r = 0.05$, $\sigma = 0.2$, $p = 0.5$, $\eta = \theta = 30$ and $T = 1$. The inversion algorithm parameters are $v_1 = 2.5$, $v_2 = 3$, $C_1 = 8$, $C_2 = 4$, $N_1 = 1500$ and $N_2 = 400$ for the top panel, and $v_1 = v_2 = 3$, $x_1 = 1$, $C_1 = 4$, $C_2 = 3$, $N_1 = 700$ and $N_2 = 1000$ for the bottom panel. It takes around 2.6 seconds and 2.9 seconds to generate one numerical price for the barrier option price and the probability, respectively, via our algorithm

Pricing up-and-in call barrier options under the DEM

K	λ	Cai & Shi	UB of disc. err.	UB of trunc. err.	KPW	Abs. err.
	0.5	9.64681	6.0E-5	7.9E-4	9.64680	0.00001
101	1.0	9.75756	6.4E-5	7.3E-4	9.75755	0.00001
	2.0	9.97456	7.1E-5	7.1E-4	9.97456	0.00000
	0.5	7.98683	6.4E-5	7.1E-4	7.98683	0.00000
105	1.0	8.09581	6.7E-5	6.6E-4	8.09581	0.00000
	2.0	8.30966	7.4E-5	6.3E-4	8.30966	0.00000
	0.5	6.47897	6.7E-5	6.4E-4	6.47897	0.00000
109	1.0	6.58585	7.1E-5	5.9E-4	6.58586	−0.00001
	2.0	6.79587	7.8E-5	5.7E-4	6.79588	−0.00001

Evaluating $P(\tau_b \le x_1, X_T \ge -x_2)$ under the DEM

x_2	Cai & Shi	UB of disc. err.	UB of trunc. err.	MC values (Std. err.)	Abs. err.
−0.5	0.01020	6.9E-6	1.2E-5	0.01069 (0.00043)	−0.00049
−0.3	0.09095	6.8E-6	2.1E-5	0.09082 (0.00098)	0.00013
−0.1	0.35480	6.7E-6	3.6E-5	0.35345 (0.00130)	0.00135
0.1	0.51205	2.4E-7	6.6E-5	0.50981 (0.00155)	0.00224
0.3	0.53686	2.2E-7	1.3E-4	0.53471 (0.00165)	0.00215
0.5	0.53845	2.1E-7	2.4E-4	0.53637 (0.00166)	0.00208

and financial engineering. Our future research topics include the study of inversion algorithms with computable error bounds for two-dimensional, two-sided Z-transforms and the mixed Z-Laplace transforms.

Acknowledgements The first author's research was supported by the GRF of the Hong Kong RGC (Project number: 610711).

TABLE 13

Evaluating two deltas $\Delta_1(\vec{u})$ and $\Delta_2(\vec{u})$ of spread options under the BSM and VG model. The column "Cai & Shi" denotes numerical results obtained via our algorithm, while "MC values" and "Std. err." are Monte Carlo estimates obtained by simulating 10^7 samples, and their associated standard errors, respectively. Related parameters for the inversion algorithm are $C_1 = 6$, $C_2 = 3$, $N_1 = N_2 = 300$, $v_1 = 7$, and $v_2 = -2$ for the BSM, and $C_1 = 6$, $C_2 = 2$, $N_1 = 300$, $N_2 = 400$, $v_1 = 7$, and $v_2 = -2$ for the VG model. All model parameters are the same as in Table 8 for the BSM and in Table 9 for the VG. It takes around 0.7 seconds to produce one numerical result via our algorithm

Evaluating the delta $\Delta_1(\vec{u})$ of spread options under the two-dimensional BSM

K	Cai & Shi	UB of disc. err.	UB of trunc. err.	MC values	Std. err.	Abs. err.
0.8	0.579294	8.9E-7	3.2E-13	0.579159	0.000133	0.000135
1.6	0.562677	8.9E-7	5.1E-18	0.562609	0.000134	0.000068
2.4	0.546017	8.9E-7	2.6E-21	0.545980	0.000135	0.000037
3.2	0.529348	8.9E-7	6.1E-24	0.529352	0.000136	−0.000004
4.0	0.512705	8.9E-7	3.6E-26	0.512674	0.000137	0.000031

Evaluating the delta $\Delta_1(\vec{u})$ of spread options under the two-dimensional VG model

K	Cai & Shi	UB of disc. err.	UB of trunc. err.	MC values	Std. err.	Abs. err.
2.4	0.577788	2.5E-9	1.3E-7	0.577762	0.000177	0.000026
2.8	0.570967	1.5E-9	5.6E-8	0.570981	0.000178	−0.000014
3.2	0.564124	1.0E-9	2.8E-8	0.564119	0.000178	−0.000001
3.6	0.557263	8.7E-10	1.5E-8	0.557267	0.000178	−0.000004
4.0	0.550386	8.7E-10	8.6E-9	0.550459	0.000179	−0.000083

Evaluating the delta $\Delta_2(\vec{u})$ of spread options under the two-dimensional BSM

K	Cai & Shi	UB of disc. err.	UB of trunc. err.	MC values	Std. err.	Abs. err.
0.8	-0.514821	7.0E-8	3.3E-12	−0.514699	0.000121	−0.000122
1.6	−0.497716	4.1E-9	1.4E-16	−0.497663	0.000122	−0.000053
2.4	−0.480702	7.7E-10	1.2E-19	−0.480681	0.000122	−0.000021
3.2	−0.463812	2.4E-10	4.5E-22	−0.463832	0.000122	0.000020
4.0	−0.447079	9.5E-11	3.6E-24	−0.447063	0.000122	−0.000016

Evaluating the delta $\Delta_2(\vec{u})$ of spread options under the two-dimensional VG model

K	Cai & Shi	UB of disc. err.	UB of trunc. err.	MC values	Std. err.	Abs. err.
2.4	−0.490498	7.0E-9	2.6E-7	−0.490499	0.000150	0.000001
2.8	−0.483567	6.5E-9	1.1E-7	−0.483609	0.000150	0.000042
3.2	−0.476642	8.4E-9	4.9E-8	−0.476664	0.000150	0.000022
3.6	−0.469725	1.3E-8	2.4E-8	−0.469756	0.000150	0.000031
4.0	−0.462818	2.0E-8	1.3E-8	−0.462917	0.000150	0.000099

APPENDIX A: PROOF OF THEOREM 2.3

PROOF. In fact, it suffices to prove (4) in the special case of $C_1 = C_2 = 0$, i.e.,

$$f(\vec{t}) = \frac{e^{\vec{v}\cdot\vec{t}}}{4|t_1t_2|}\sum_{\vec{k}\in\mathbb{Z}^2}(-1)^{k_1+k_2}\Re\left(L_f\left(v_1+i\frac{k_1\pi}{t_1}, v_2+i\frac{k_2\pi}{t_2}\right)\right) - \sum_{\vec{k}\in\mathbb{Z}^2\setminus\{\vec{0}\}} e^{-2\vec{v}\circ\vec{k}\circ\vec{t}} f((2\vec{k}+1)\circ\vec{t}). \tag{26}$$

If $C_1 \neq 0$ or $C_2 \neq 0$, we can obtain (4) immediately by applying (26) to a new function $f^*(\vec{y}) := f(\vec{y} - \mathrm{sgn}(\vec{t})\circ\vec{C})$ at the point $\vec{t} + \mathrm{sgn}(\vec{t})\circ\vec{C}$.

Define $g(t) := e^{-\vec{v}\cdot\vec{t}} f(\vec{t})$. Then to prove (26) under the assumption $t_1t_2 \neq 0$, it is equivalent to showing the following two-dimensional Poisson summation formula.

$$\sum_{\vec{k}\in\mathbb{Z}^2} g(t_1+2k_1|t_1|, t_2+2k_2|t_2|) = \frac{1}{4|t_1t_2|}\sum_{\vec{k}\in\mathbb{Z}^2}(-1)^{k_1+k_2} L_f\left(v_2+i\frac{k_1\pi}{|t_1|}, v_2+i\frac{k_2\pi}{|t_2|}\right). \tag{27}$$

Introduce a new function

$$g_p(\vec{x}) := \sum_{\vec{l}\in\mathbb{Z}^2} g\Big(2|t_1|(x_1+l_1), 2|t_2|(x_2+l_2)\Big), \text{ with } g_p(\vec{x}+\vec{l}) \equiv g_p(\vec{x})\ \forall\, \vec{l}\in\mathbb{Z}^2.$$

We point out that $g_p(\frac{1}{2},\frac{1}{2})$ is exactly the LHS of (27). Now we shall prove that the RHS of (27) is exactly the Fourier series of $g_p(\frac{1}{2},\frac{1}{2})$, and moreover, it converges to $g_p(\frac{1}{2},\frac{1}{2})$. This can be obtained immediately by Proposition 3.3.2 in Grafakos [16] if we can verify the following three conditions: (a) $g_p(\vec{x})$ is continuous at the point $(\frac{1}{2},\frac{1}{2})$; (b) $g_p(\vec{x}) \in L^1([0,1]\times[0,1])$; and (c) the partial sum of the Fourier series of $g_p(\vec{x})$ converges at the point $(\frac{1}{2},\frac{1}{2})$. Let us verify (a), (b), and (c) one by one.

As for (a), we claim that $g_p(\vec{x})$ is continuous on $\mathbb{R}^2$. Indeed, consider a sequence $\vec{x}^{(n)} := (x_1^{(n)}, x_2^{(n)}) \to \vec{x}$ and assume $|\vec{x}^{(n)} - \vec{x}| < 1$ without loss of generally. Then by (3) we obtain that for any $\vec{l}\in\mathbb{Z}^2$,

$$\begin{aligned} g\Big(2|\vec{t}|\circ(\vec{x}^{(n)}+\vec{l})\Big) &\le \kappa e^{-2c_1|t_1|\cdot|x_1^{(n)}+l_1|-2c_2|t_2|\cdot|x_2^{(n)}+l_2|} \\ &\le \kappa e^{-2c_1|t_1l_1|-2c_2|t_2l_2|} e^{2c_1|t_1|(|x_1|+1)+2c_2|t_2|(|x_2|+1)} =: g^*(\vec{l}), \end{aligned}$$

with $\sum_{\vec{l}\in\mathbb{Z}^2} g^*(\vec{l}) < +\infty$. Applying the dominated convergence theorem yields $g_p(\vec{x}) = \lim_{n\to+\infty} g_p(\vec{x}^{(n)})$.

The condition (b) is also satisfied because

$$\begin{aligned}(28)\qquad \int_0^1\int_0^1 |g_p(\vec{x})|dx_1dx_2 &\le \int_0^1\int_0^1 \sum_{\vec{l}\in\mathbb{Z}^2} \left|g\Big(2|\vec{t}| \circ (\vec{x}+\vec{l})\Big)\right| dx_1dx_2\\ &= \sum_{\vec{l}\in\mathbb{Z}^2} \int_0^1\int_0^1 \left|g\Big(2|\vec{t}| \circ (\vec{x}+\vec{l})\Big)\right| dx_1dx_2\\ &= \int_{-\infty}^{+\infty}\int_{-\infty}^{+\infty} \left|g(2|\vec{t}| \circ \vec{x})\right| dx_1dx_2\\ &= \frac{1}{4|t_1t_2|}\int_{-\infty}^{+\infty}\int_{-\infty}^{+\infty} |g(\vec{x})|\, dx_1dx_2 < +\infty.\end{aligned}$$

To show that (c) also holds, we calculate the Fourier coefficients of $g_p(\vec{x})$ as follows.

$$\begin{aligned}c_{\vec{k}}(\vec{x}) &= \int_0^1\int_0^1 g_p(x)e^{-2\pi i\vec{k}\cdot\vec{x}}dx_1dx_2\\ &= \sum_{\vec{l}\in\mathbb{Z}^2}\int_0^1\int_0^1 g\Big(2|\vec{t}| \circ (\vec{x}+\vec{l})\Big)e^{-2\pi i\vec{k}\cdot\vec{x}}dx_1dx_2\\ &= \int_{-\infty}^{+\infty}\int_{-\infty}^{+\infty} g\Big(2|\vec{t}| \circ \vec{x}\Big)e^{-2\pi i\vec{k}\cdot\vec{x}}dx_1dx_2\\ &= \frac{1}{4|t_1t_2|}\int_{-\infty}^{+\infty}\int_{-\infty}^{+\infty} g(\vec{x})e^{-i\left(\frac{k_1\pi x_1}{|t_1|}+\frac{k_2\pi x_2}{|t_2|}\right)}dx_1dx_2\\ &= \frac{1}{4|t_1t_2|}L_f\left(v_1+i\frac{k_1\pi}{|t_1|}, v_2+i\frac{k_2\pi}{|t_2|}\right),\end{aligned}$$

where the second equality holds due to (28) and Fubini's Theorem. Accordingly, for any fixed $\vec{x}\in\mathbb{R}^2$, the partial sum $S_{\vec{N}}(\vec{x})$ of the Fourier series of $g_p(\vec{x})$ is given by

$$S_{\vec{N}}(\vec{x}) = \frac{1}{4|t_1t_2|}\sum_{k_1=-N_1}^{N_1}\sum_{k_2=-N_2}^{N_2} L_f\left(v_1+i\frac{k_1\pi}{|t_1|}, v_2+i\frac{k_2\pi}{|t_2|}\right)e^{2\pi i\vec{k}\cdot\vec{x}}.$$

As N_1 and N_2 tend to $+\infty$, the double series $S_{\vec{N}}(\vec{x})$ is absolutely convergent because of Assumption 2.2. This implies that (c) also holds. □

APPENDIX B: PROOF OF THEOREM 3.1, PROPOSITION 3.2 AND PROPOSITION 3.3

PROOF OF THEOREM 3.1. Our proof is focused only on the case: $t_1 \geq 0$ and $t_2 \geq 0$. Other cases can be treated similarly and are thus omitted. First of all, we know from (7) that

$$|e_D(\vec{t},\vec{v},\vec{C})| \leq \sum_{\vec{k}\in\mathbb{Z}^2\setminus\{\vec{0}\}} e^{-2(\vec{v}\circ\vec{k})\cdot(\vec{t}+\vec{C}\circ sgn(\vec{t}))}|f(\vec{t}+2\vec{k}\circ(\vec{t}+\vec{C}\circ sgn(\vec{t})))|.$$

Divide the region of $\vec{k}$, i.e., $\mathbb{Z}^2\setminus\{\vec{0}\}$, into eight disjoint subregions

$$A_1=\mathbb{Z}^+\times\mathbb{Z}^+,\quad A_2=\mathbb{Z}^-\times\mathbb{Z}^+,\quad A_3=\mathbb{Z}^-\times\mathbb{Z}^-,\quad A_4=\mathbb{Z}^+\times\mathbb{Z}^-,$$
$$B_1=\{0\}\times\mathbb{Z}^+,\quad B_2=\{0\}\times\mathbb{Z}^-,\quad B_3=\mathbb{Z}^+\times\{0\},\quad B_4=\mathbb{Z}^-\times\{0\}.$$

By (8) we obtain

$$|f(\vec{x})| \leq \begin{cases} \delta(l_1^*,l_2^*)e^{l_1^*x_1+l_2^*x_2} & \text{when } x_1\geq 0, x_2\geq 0;\\ \delta(u_1^*,l_2^*)e^{u_1^*x_1+l_2^*x_2} & \text{when } x_1< 0, x_2\geq 0;\\ \delta(u_1^*,u_2^*)e^{u_1^*x_1+u_2^*x_2} & \text{when } x_1< 0, x_2< 0;\\ \delta(l_1^*,u_2^*)e^{l_1^*x_1+u_2^*x_2} & \text{when } x_1\geq 0, x_2< 0. \end{cases}$$

Note that $2k_j(t_j+C_jsgn(t_j))+t_j$ always has the same sign with k_j. Then

$$\begin{aligned}\sum_{A_1} &:= \sum_{\vec{k}\in A_1} \exp^{-2(\vec{v}\circ\vec{k})\cdot(\vec{t}+\vec{C}\circ sgn(\vec{t}))}\,|f(\vec{t}+2\vec{k}\circ(\vec{t}+\vec{C}\circ sgn(\vec{t})))|\\ &\leq \delta(l_1^*,l_2^*)\sum_{k_1=1}^{+\infty}\sum_{k_2=1}^{+\infty}\Big[e^{-2k_1(t_1+C_1)v_1-2k_2(t_2+C_2)v_2}\\ &\qquad\qquad\times e^{l_1^*(2k_1(t_1+C_1)+t_1)+l_2^*(2k_2(t_2+C_2)+t_2)}\Big]\\ &= \delta(l_1^*,l_2^*)e^{(3l_1^*-2v_1)t_1+(3l_2^*-2v_2)t_2}\frac{e^{-2C_1(v_1-l_1^*)}}{1-e^{-2(t_1+C_1)(v_1-l_1^*)}}\frac{e^{-2C_2(v_2-l_2^*)}}{1-e^{-2(t_2+C_2)(v_2-l_2^*)}}\\ &\leq \delta(l_1^*,l_2^*)e^{(3l_1^*-2v_1)t_1+(3l_2^*-2v_2)t_2}\frac{1}{e^{2d_1C_1}-1}\frac{1}{e^{2d_2C_2}-1}.\end{aligned}$$

Similarly, it can be shown that

$$\sum_{A_2} \leq \delta(u_1^*,l_2^*)e^{(2v_1-u_1^*)t_1+(3l_2^*-2v_2)t_2}\frac{1}{e^{2d_1C_1}-1}\frac{1}{e^{2d_2C_2}-1},$$
$$\sum_{A_3} \leq \delta(u_1^*,u_2^*)e^{(2v_1-u_1^*)t_1+(2v_2-u_2^*)t_2}\frac{1}{e^{2d_1C_1}-1}\frac{1}{e^{2d_2C_2}-1},$$

$$\sum_{A_4} \le \delta(l_1^*, u_2^*) e^{(3l_1^* - 2v_1)t_1 + (2v_2 - u_2^*)t_2} \frac{1}{e^{2d_1C_1} - 1} \frac{1}{e^{2d_2C_2} - 1},$$

$$\sum_{B_1} \le \frac{\delta(l_1^*, l_2^*) e^{3l_2^* - 2v_2}}{e^{2d_2C_2} - 1}, \quad \sum_{B_2} \le \frac{\delta(l_1^*, u_2^*) e^{2v_2 - u_2^*}}{e^{2d_2C_2} - 1},$$

$$\sum_{B_3} \le \frac{\delta(l_1^*, l_2^*) e^{3l_1^* - 2v_1}}{e^{2d_1C_1} - 1}, \quad \sum_{B_4} \le \frac{\delta(u_1^*, l_2^*) e^{2v_1 - u_1^*}}{e^{2d_1C_1} - 1}.$$

Adding the eight inequalities above together completes the proof. □

Proof of Proposition 3.2. By the Bromwich contour integral we obtain

$$\begin{aligned} e^{-\vec{y}\cdot\vec{t}} |f(\vec{t})| &= \frac{e^{-\vec{y}\cdot\vec{t}}}{4\pi^2} \left| \int_{-\infty}^{+\infty} \int_{-\infty}^{+\infty} e^{(\vec{y} + i\vec{\omega})\cdot\vec{t}} L_f(\vec{y} + i\vec{\omega}) d\omega_1 d\omega_2 \right| \\ &\le \frac{1}{4\pi^2} \int_{-\infty}^{+\infty} \int_{-\infty}^{+\infty} |L_f(\vec{y} + i\vec{\omega})| d\omega_1 d\omega_2, \end{aligned}$$

which justifies Proposition 3.2 immediately. □

Proof of Proposition 3.3. Since the ROAC is defined to be the interior of the set (2), there exists $\epsilon > 0$ such that $[v_1 - \epsilon, v_1 + \epsilon] \times [v_2 - \epsilon, v_2 + \epsilon] \subset$ ROAC of $L_f(\vec{s})$. Then for any $\vec{v}$ in ROAC, (8) implies (3) with parameters $\kappa = \max\{\delta(v_1 + \epsilon, v_2 + \epsilon), \delta(v_1 + \epsilon, v_2 - \epsilon), \delta(v_1 - \epsilon, v_2 + \epsilon), \delta(v_1 - \epsilon, v_2 - \epsilon)\}$ and $c_1 = c_2 = \epsilon$. □

APPENDIX C: PROOF OF THEOREM 4.1

Proof. From (6) we know

$$|e_T(\vec{t}, \vec{v}, \vec{C}, \vec{N})| \le \frac{e^{\vec{v}\cdot\vec{t}}}{4(|t_1| + C_1)(|t_2| + C_2)} \sum_{\vec{k} \in \mathbb{Z}^2 \setminus D_0^{\vec{N}}} |L_f(\vec{v} + i\vec{a} \circ \vec{k})|.$$

(i) If $L_f(\vec{v} + i\vec{\omega})$ satisfies (13), simple algebra yields

$$\begin{aligned} \sum_{D_1} &:= \sum_{\vec{k} \in \mathbb{Z}^2 \cap D_1^{\vec{N}}} |L_f(\vec{v} + i\vec{a} \circ \vec{k})| \\ &\le 2 \sum_{k_2 = -N_2}^{N_2} \zeta_2(\vec{v}, b_2 k_2 sgn(t_2)) \sum_{k_1 = N_1 + 1}^{+\infty} (b_1 k_1)^{-\alpha_1} \\ &\le 2 \sum_{k_2 = -N_2}^{N_2} \zeta_2(\vec{v}, b_2 k_2 sgn(t_2)) \int_{N_1}^{+\infty} x^{-\alpha_1} dx \end{aligned}$$

$$= 2 \sum_{k_2=-N_2}^{N_2} \zeta_2(\vec{v}, b_2 k_2 sgn(t_2)) b_1^{-\alpha_1} \frac{N_1^{1-\alpha_1}}{\alpha_1 - 1}.$$

Similarly, we can obtain

$$\sum_{D_2} := \sum_{\vec{k} \in \mathbb{Z}^2 \cap D_2^{\vec{N}}} |L_f(\vec{v} + i\vec{a} \circ \vec{k})| \le 2 \sum_{k_1=-N_1}^{N_1} \zeta_1(\vec{v}, b_1 k_1 sgn(t_1)) b_2^{-\alpha_2} \frac{N_2^{1-\alpha_2}}{\alpha_2 - 1},$$

$$\sum_{D_3} := \sum_{\vec{k} \in \mathbb{Z}^2 \cap D_3^{\vec{N}}} |L_f(\vec{v} + i\vec{a} \circ \vec{k})| \le 4\zeta(\vec{v}) \sum_{k_1=N_1+1}^{+\infty} \sum_{k_2=N_2+1}^{+\infty} (b_1 k_1)^{-\alpha_3} (b_2 k_2)^{-\alpha_4}$$

$$\le 4\zeta(\vec{v}) b_1^{-\alpha_3} \frac{N_1^{1-\alpha_3}}{\alpha_3 - 1} b_2^{-\alpha_4} \frac{N_2^{1-\alpha_4}}{\alpha_4 - 1}.$$

Then (14) follows immediately.

(ii) Similarly to (i), if $L_f(\vec{v} + i\vec{\omega})$ satisfies (15), we have

$$\sum_{D_1} \le 2 \sum_{k_2=-N_2}^{N_2} \zeta_2(\vec{v}, b_2 k_2 sgn(t_2)) \sum_{k_1=N_1+1}^{+\infty} (b_1 k_1)^{-\alpha_1} e^{-\rho_1 (b_1 k_1)^{\xi_1}}$$

$$\le 2 \sum_{k_2=-N_2}^{N_2} \zeta_2(\vec{v}, b_2 k_2 sgn(t_2)) \int_{N_1}^{+\infty} x^{-\alpha_1} e^{-\rho_1 (b_1 x)^{\xi_1}} dx$$

$$= 2 \sum_{k_2=-N_2}^{N_2} \zeta_2(\vec{v}, b_2 k_2 sgn(t_2)) \frac{\Gamma(\frac{1-\alpha_1}{\xi_1}, \rho_1 b_1^{\xi_1} N_1^{\xi_1})}{b_1 \xi_1} \rho_1^{\frac{\alpha_1 - 1}{\xi_1}},$$

where the second inequality holds because the function $x^{-\alpha_j} e^{-\rho_j x^{\xi_j}}$ is decreasing in x when $x \ge (\frac{\max\{-\alpha_j, 0\}}{\xi_j \rho_j})^{\frac{1}{\xi_j}}$. Similarly,

$$\sum_{D_2} \le 2 \sum_{k_1=-N_1}^{N_1} \zeta_1(\vec{v}, b_1 k_1 sgn(t_1)) \frac{\Gamma(\frac{1-\alpha_2}{\xi_2}, \rho_2 b_2^{\xi_2} N_2^{\xi_2})}{b_2 \xi_2} \rho_2^{\frac{\alpha_2 - 1}{\xi_2}},$$

$$\sum_{D_3} \le 4\zeta(\vec{v}) \frac{\Gamma(\frac{1-\alpha_3}{\xi_3}, \rho_3 b_1^{\xi_3} N_1^{\xi_3})}{b_1 \xi_3} \rho_3^{\frac{\alpha_3 - 1}{\xi_3}} \frac{\Gamma(\frac{1-\alpha_4}{\xi_4}, \rho_4 b_2^{\xi_4} N_2^{\xi_4})}{b_2 \xi_4} \rho_4^{\frac{\alpha_4 - 1}{\xi_4}}.$$

Thus (16) is proved. □

APPENDIX D: PROOF OF PROPOSITION 5.1 AND PROPOSITION 5.3

Proof of Proposition 5.1. The proof of (ii) is straightforward according to Table 1. As for (i), $F(\cdot)$ is continuous because $\vec{X}(T)$ has a continuous

distribution. Besides, applying the dominated convergence theorem and using the fact that $Ee^{X_1(T)} < +\infty$ yields that $\mathrm{Spr}(\cdot)$ is also continuous. Finally, it is straightforward and elementary to verify that $F(\cdot)$ and $\mathrm{Spr}(\cdot)$ satisfy (3) thanks to the assumption that $\vec{0}$ belongs to the ROAC and the details are thus omitted. □

PROOF OF PROPOSITION 5.3. Since $\alpha \in (0,1)$ and $\lambda > 0$, we obtain from (20) that

$$\begin{aligned}
|L_f(\vec{s})| &= \left(\frac{a_- - s_1 - s_2}{a_-} \cdot \frac{a_+ + s_1 + s_2}{a_+}\right)^{-\alpha\lambda T} \\
&\quad \times \prod_{j=1}^{2} \left(\frac{a_- - s_j}{a_-} \cdot \frac{a_+ + s_j}{a_+}\right)^{-(1-\alpha)\lambda T} \\
&\le \left(\frac{a_- - v_1 - v_2}{a_-} \cdot \frac{a_+ + v_1 + v_2}{a_+}\right)^{-\alpha\lambda T} \\
&\quad \times \prod_{j=1}^{2} \left(\frac{\max\{(a_- - v_j)\cdot(a_+ + v_j), |\omega_j|^2\}}{a_- a_+}\right)^{-(1-\alpha)\lambda T} \\
&= \zeta(\vec{v}) \prod_{j=1}^{2} \left(\max\left\{(a_- - v_j)\cdot(a_+ + v_j), |\omega_j|^2\right\}\right)^{-(1-\alpha)\lambda T},
\end{aligned}$$

which completes the proof. □

APPENDIX E: THE SPECIAL CASE $K = 0$ OF SPREAD OPTIONS UNDER THE BSM

When $K = 0$, the spread option under the two-dimensional BSM becomes analytically tractable. Indeed, if we define a new measure $\hat{\mathbb{P}}$

$$\frac{d\hat{\mathbb{P}}}{d\mathbb{P}} = e^{-(r-q_2)T} \frac{S_2(T)}{S_2(0)},$$

then by change of measure we obtain a closed-form spread option price as follows

$$\begin{aligned}
e^{-rT} E[(S_1(T) - S_2(T))^+] &= S_2(0) e^{-q_2 T} \hat{E}\left[\left(\frac{S_1(T)}{S_2(T)} - 1\right)^+\right] \\
&= S_2(0) e^{-q_2 T}\left[e^{\tilde{\mu} + \frac{\tilde{\sigma}^2}{2}} \Phi\left(\frac{\tilde{\mu}}{\tilde{\sigma}} + \tilde{\sigma}\right) - \Phi\left(\frac{\tilde{\mu}}{\tilde{\sigma}}\right)\right], \qquad (29)
\end{aligned}$$

where $\tilde{\mu} = x_1(0) - x_2(0) - (q_1 - q_2)T - \tilde{\sigma}^2/2$, $\tilde{\sigma} = \sqrt{(\sigma_1^2 + \sigma_2^2 - 2\sigma_1\sigma_2\rho)T}$, $\Phi(\cdot)$ denotes the standard normal cdf, and the second equality holds because

$S_1(T)/S_2(T)$ is still log-normally distributed under the new measure $\hat{\mathbb{P}}$. In fact, (29) is essentially the Black-Scholes formula.

When $K = 0$, the Laplace transform of the spread option price also becomes simpler. Indeed, the single Laplace transform w.r.t. $X_2(0)$ has a closed-form expression. Specifically, defining $\mathrm{Spr}(x) := e^{-rT}E[(e^{x_1(0)+X_1(T)} - e^{x+X_2(T)})^+]$, then we have

$$\begin{aligned} L_{\mathrm{Spr}}(s) &:= \int_{-\infty}^{+\infty} e^{-sx}\mathrm{Spr}(x)dx \\ &= e^{-rT}E\left[\int_{-\infty}^{x_1(0)+X_1(T)-X_2(T)} e^{-sx}(e^{x_1(0)+X_1(T)} - e^{x+X_2(T)})dx\right] \\ &= \frac{e^{-rT+(1-s)x_1(0)}}{s(s-1)}E[e^{-(s-1)X_1(T)+sX_2(T)}] \\ &= \frac{e^{-rT+(1-s)x_1(0)}}{s(s-1)}L_f(s-1,-s) < +\infty, \end{aligned} \tag{30}$$

for all $s \equiv v + i\omega$ with $v \equiv \Re(s) < 0$, where $L_f(\cdot,\cdot)$ is given by (19) and the second equality follows from Fubini's Theorem.

Then the one-dimensional, two-sided Euler inversion algorithm applies to evaluate the spread option price $\mathrm{Spr}(x)$ as a special case of our two-dimensional algorithm. Moreover, the related discretization and truncation error bounds can be derived similarly (see also Cai et al [7]). More precisely, note that for all $v < 0$ and $\omega \neq 0$,

$$|L_{\mathrm{Spr}}(s)| = \left|\frac{e^{-rT+(1-v-i\omega)x_1(0)}}{(v+i\omega)(v-1+i\omega)}\right| \cdot |L_f(s-1,-s)| \leq \frac{\zeta(v)}{|\omega|^2}e^{-\hat{\rho}|\omega|^2},$$

where $\hat{\rho} = (\sigma_1^2 + \sigma_2^2 - 2\sigma_1\sigma_2\rho)T/2$ and

$$\begin{aligned} \zeta(v) := \exp\big\{ &-rT + (1-v)x_1(0) + (1-v)(r - q_1 - \sigma_1^2/2)T \\ &+ v(r - q_2 - \sigma_2^2/2)T + ((v-1)^2\sigma_1^2 + v^2\sigma_2^2)T/2 + (1-v)v\sigma_1\sigma_2\rho T\big\}. \end{aligned}$$

Then adapting Theorem 4.1 for the one-dimensional case (or applying Theorem 5.1 in Cai et al [7] directly) yields the following truncation error bound

$$|e_T(x,v,C,N)| \leq \frac{\zeta(v)e^{vt}\sqrt{\hat{\rho}}}{2\pi} \cdot \Gamma\left(-\frac{1}{2}, \frac{\hat{\rho}\pi^2N^2}{(|t|+C)^2}\right).$$

Besides, to control the discretization error, we need to first specify a similar function $\delta(\cdot)$ as in (8). Analogously to Section 3.2.1, we can specify $\delta(\cdot)$ in

the following way.

$$
\begin{aligned}
&e^{-yx}|\mathrm{Spr}(x)| \\
&= \frac{e^{-yx}}{2\pi}\left|\int_{-\infty}^{+\infty} e^{(y+i\omega)x} L_{\mathrm{Spr}}(y+i\omega)d\omega\right| \le \frac{1}{2\pi}\int_{-\infty}^{+\infty} |L_{\mathrm{Spr}}(y+i\omega)|d\omega \\
&= \frac{1}{2\pi}\left[\int_{-\infty}^{-1} |L_{\mathrm{Spr}}(y+i\omega)|d\omega + \int_{-1}^{1}\left|\int_{-\infty}^{+\infty} e^{-(y+i\omega)x}\mathrm{Spr}(x)dx\right| d\omega \right. \\
&\qquad \left. + \int_{1}^{+\infty} |L_{\mathrm{Spr}}(y+i\omega)|d\omega\right] \\
&\le \frac{\zeta(y)}{\pi}\int_{1}^{+\infty}\frac{1}{\omega^2}e^{-\hat{\rho}\omega^2}d\omega + \frac{1}{2\pi}\int_{-1}^{1}\int_{-\infty}^{+\infty} e^{-yx}\mathrm{Spr}(x)dxd\omega \\
&= \frac{\zeta(y)\sqrt{\hat{\rho}}}{2\pi}\Gamma\left(-\frac{1}{2},\hat{\rho}\right) + \frac{1}{\pi}L_{\mathrm{Spr}}(y) =: \delta(y), \quad \text{for any } y<0 \text{ and } x\in\mathbb{R}.
\end{aligned}
$$

Then adapting Theorem 3.1 for the one-dimensional case (or applying Theorem 4.1 in Cai et al [7] directly) yields the following discretization error bound

$$|e_D(x,v,C)| \le \frac{\rho(v,x)}{e^{\theta(v)C}-1},$$

for any $v\in(\sigma_l^*,\sigma_u^*)$, where $\sigma_l^*<\sigma_u^*<0$, $\theta(v):=2\cdot\min\{\sigma_u^*-v, v-\sigma_l^*\}>0$, and

$$\rho(v,x) := \begin{cases} \delta(\sigma_u^*)e^{(2v-\sigma_u^*)x} + \delta(\sigma_l^*)e^{(3\sigma_l^*-2v)x}, & \text{if } x\ge 0, \\ \delta(\sigma_l^*)e^{(2v-\sigma_l^*)x} + \delta(\sigma_u^*)e^{(3\sigma_u^*-2v)x}, & \text{if } x<0. \end{cases}$$

APPENDIX F: PROOF OF PROPOSITION 6.1

Proof. The argument of (ii) is straightforward according to Table 4 and Proposition 6.2 in Section 6.3. As regards (i), it follows from Proposition 3.3 that both $F_{\tau_b,X_T}(\cdot)$ and $\mathrm{UIC}(\cdot)$ satisfy (3) because in Section 6.2 we succeed in finding the functions $\delta(\vec{v})$ that satisfy (8) for any $\vec{v}$ in their respective ROACs. Therefore, what is left is to verify the continuity of $F_{\tau_b,X_T}(\cdot)$ and $\mathrm{UIC}(\cdot)$. Define two sets $A:=\{\text{The process } \{X_t\} \text{ jumps at time } T\}$ and $B:=\{\tau_b=T\}$. It is easy to see that $P(A)=P(B)=0$ under the DEM. Then for any $\vec{\delta}\in\mathbb{R}^2$, as $\vec{\delta}\to 0$, we have

$$
\begin{aligned}
\mathrm{UIC}(T+\delta_1,k+\delta_2) &= e^{-r(T+\delta_1)}E\left[(S_0e^{X_{T+\delta_1}}-e^{-k-\delta_2})^+1_{\{\tau_b<T+\delta_1\}}\right] \\
&= e^{-r(T+\delta_1)}E\left[(S_0e^{X_{T+\delta_1}}-e^{-k-\delta_2})^+1_{\{\tau_b<T+\delta_1\}}\cdot 1_{A^c\cap B^c}\right], \\
&\to e^{-rT}E\left[(S_0e^{X_T}-e^{-k})^+1_{\{\tau_b<T\}}\cdot 1_{A^c\cap B^c}\right] = \mathrm{UIC}(T,k),
\end{aligned}
$$

where the second and third equalities hold because $P(A\cup B)=0$, and the "$\to$" holds due to the dominated convergence theoremand and the continuity

of the function $(S_0e^{X_T}-e^{-k})^+1_{\{\tau_b<T\}}$ in T and k on the set $A^c\cap B^c$. This implies that UIC$(\cdot)$ is a continuous function. The continuity of $F_{\tau_b,X_T}(\cdot)$ can be shown similarly and is omitted. □

APPENDIX G: PROOF OF PROPOSITION 6.2

To prove Proposition 6.2, we first present the following three lemmas.

LEMMA G.1. *For any fixed* $v_1=\Re(s_1)>\max\{G(v_2),0\}$ *and* $v_2=\Re(s_2)\in(-\theta,\eta)$, *we have*

$$\begin{aligned}&\textit{(i)}\ |s_1-G(s_2)|\ge\hat\zeta|\omega_1| \quad \textit{for all } \vec\omega\in D_1^{\vec M^*};\\ &\textit{(ii)}\ |s_1-G(s_2)|\ge\frac{\sigma^2}{4}|\omega_2|^2 \quad \textit{for all } \vec\omega\in D_2^{\vec M^*};\\ &\textit{(iii)}\ |s_1-G(s_2)|\ge\frac{\sigma}{2}|\omega_1|^{1/2}|\omega_2| \quad \textit{for all } \vec\omega\in D_3^{\vec M^*}.\end{aligned}$$

where $\vec\omega:=(\omega_1,\omega_2)\equiv\Im(\vec s)$, $\hat\zeta:=\hat\zeta(\vec v,\omega_2)=(v_1-\Re(G(s_2)))/|v_1-G(s_2)|$, *for* $v_1\ne G(s_2)$ *and* $\hat\zeta=1$ *for* $v_1=G(s_2)$,

$$\vec M^*:=(M_1^*,M_2^*),\quad M_1^*=\left(\frac{5\lambda}{\sigma M_2^*}\right)^2\left(\frac{c_2}{M_2^*}+1\right)^2,\quad \textit{and}$$

$$M_2^*=\max\left\{\sqrt{\frac{4}{\sigma^2}(\lambda+|c_1|)+\left(\frac{4}{\sigma^2}\lambda c_2\right)^{2/3}},\frac{2\sqrt2}{\sigma^2}\times\sqrt{(\sigma^2v_2+\mu)^2+|c_1|\sigma^2}\right\}.$$

Here $c_1:=v_1-\frac12\sigma^2v_2^2-\mu v_2$ *and* $c_2:=\eta p+\theta q$.

PROOF. Indeed, (i) holds for all $\vec\omega\in\mathbb{R}^2$. If $\Im(G(s_2))=0$, (i) can be obtained immediately because $\hat\zeta=1$ and $|s_1-G(s_2)|\ge|\omega_1|$. If $\Im(G(s_2))\ne0$, then we have $\hat\zeta<1$ and (i) also holds because

$$\begin{aligned}|s_1-G(s_2)|&=\sqrt{(v_1-\Re(G(s_2)))^2+(\omega_1-\Im(G(s_2)))^2}\\&=\sqrt{\hat\zeta^2\omega_1^2+\left(\omega_1\sqrt{1-\hat\zeta^2}-\Im(G(S_2))/\sqrt{1-\hat\zeta^2}\right)^2}\ge\hat\zeta|\omega_1|.\end{aligned}$$

Now let us prove (ii). For any $\vec\omega\in D_2^{\vec M^*}$, some algebra yields

(31)

$$\begin{aligned}&|s_1-G(s_2)|\\&\ge\left|\left(\frac{\sigma^2}{2}\omega_2^2+c_1\right)+i(\omega_1-(\sigma^2v_2+\mu)\omega_2)\right|-\left|\lambda\left(\frac{\eta p}{\eta-s_2}+\frac{\theta q}{\theta+s_2}-1\right)\right|\end{aligned}$$

$$\geq \frac{\sigma^2}{2}\omega_2^2 - |c_1| - \lambda\left(\frac{c_2}{M_2^*}+1\right) \geq \frac{\sigma^2}{4}\omega_2^2 + \frac{\sigma^2}{4}M_2^{*2} - |c_1| - \lambda\left(\frac{c_2}{M_2^*}+1\right)$$
$$= \frac{\sigma^2}{4}\omega_2^2 + \frac{\sigma^2}{4}\left[M_2^{*2} - \frac{4}{\sigma^2}(|c_1|+\lambda) - \frac{4}{\sigma^2}\frac{\lambda c_2}{M_2^*}\right],$$

where the second and third inequalities hold because $|\omega_2| > M_2^*$. Furthermore, by the definition of M_2^*, we know $M_2^* \geq \sqrt{\frac{4}{\sigma^2}(\lambda+|c_1|) + (\frac{4}{\sigma^2}\lambda c_2)^{2/3}}$. It follows that

$$M_2^{*2} - \frac{4}{\sigma^2}(|c_1|+\lambda) \geq \frac{\frac{4}{\sigma^2}\lambda c_2}{\sqrt{M_2^{*2} - \frac{4}{\sigma^2}(|c_1|+\lambda)}} > \frac{4}{\sigma^2}\frac{\lambda c_2}{M_2^*},$$

which along with (31) leads to (ii) immediately.

Finally, we shall show (iii). Similarly as in the derivation of (31), when $|\omega_2| > M_2^*$ we have

$$|s_1 - G(s_2)|$$
$$\geq \left|\left(\frac{\sigma^2}{2}\omega_2^2 + c_1\right) + i(\omega_1 - (\sigma^2 v_2 + \mu)\omega_2)\right| - \left|\lambda\left(\frac{\eta p}{\eta - s_2} + \frac{\theta q}{\theta + s_2} - 1\right)\right|$$
(32)
$$\geq \left[\left(\frac{\sigma^2}{2}\omega_2^2 + c_1\right)^2 + (\omega_1 - (\sigma^2 v_2 + \mu)\omega_2)^2\right]^{1/2} - \lambda\left(\frac{c_2}{M_2^*}+1\right).$$

By the definition of M_2^*, we know $M_2^* \geq \frac{2\sqrt{2}}{\sigma^2}\sqrt{(\sigma^2 v_2+\mu)^2 + |c_1|\sigma^2}$, which implies that $\frac{\sigma^4}{8}\omega_2^2 \geq \frac{\sigma^4}{8}M_2^{*2} \geq (\sigma^2 v_2+\mu)^2 + |c_1|\sigma^2$, for any $|\omega_2| > M_2^*$. It follows that

$$\left(\frac{\sigma^2}{2}\omega_2^2 + c_1\right)^2 + (\omega_1 - (\sigma^2 v_2+\mu)\omega_2)^2$$
$$= \frac{\sigma^4}{8}\omega_2^4 + c_1^2 + \frac{1}{2}\omega_1^2 + \frac{1}{2}(\omega_1 - 2(\sigma^2 v_2+\mu)\omega_2)^2$$
$$+ \omega_2^2\left(\frac{\sigma^4}{8}\omega_2^2 - (\sigma^2 v_2+\mu)^2 - c_1\sigma^2\right)$$
(33)
$$\geq \frac{\sigma^4}{8}\omega_2^4 + \frac{1}{2}\omega_1^2 \geq \frac{\sigma^2}{2}|\omega_1||\omega_2|^2.$$

From (32) and (33) we obtain

$$|s_1 - G(s_2)| \geq \frac{\sigma}{\sqrt{2}}|\omega_1|^{\frac{1}{2}}|\omega_2| - \lambda\left(\frac{c_2}{M_2^*}+1\right)$$
$$> \frac{\sigma}{2}|\omega_1|^{\frac{1}{2}}|\omega_2| + \frac{\sigma}{5}M_1^{*\frac{1}{2}}M_2^* - \lambda\left(\frac{c_2}{M_2^*}+1\right) = \frac{\sigma}{2}|\omega_1|^{\frac{1}{2}}|\omega_2|,$$

where the second inequality holds because $\frac{1}{\sqrt{2}} > \frac{1}{2} + \frac{1}{5}$. □

LEMMA G.2. *For any fixed $x > 0$ and $y \in \mathbb{R}$, the equation $G(z) = x + iy$ has exactly two roots with positive real parts, denoted by $\beta_{1,x+iy}$ and $\beta_{2,x+iy}$. Moreover, when $|y|$ is sufficiently large such that $|y| > Y(x)$, $\beta_{1,x+iy}$ and $\beta_{2,x+iy}$ satisfy*

$$|\beta_{1,x+iy} - \eta| \le \frac{Y_3}{|y|\theta} = O\Big(\frac{1}{|y|}\Big) \quad \text{and} \quad |\beta_{2,x+iy} - z_y| \le \frac{2|\mu|}{\sigma^2} = O(1), \tag{34}$$

where $z_y = \frac{\sqrt{|y|}}{\sigma}(1 + i \cdot sgn(y))$, $Y(x) = \max\{Y_1, Y_2, Y_3, Y_4\}$, $Y_1 = 2(\sigma\eta + \frac{2|\mu|}{\sigma})^2$, $Y_2 = \frac{1}{2}(\frac{4|\mu|}{\sigma} + \frac{\sigma}{|\mu|}(x + 2\lambda))^2$, $Y_3 = 2\eta^2\sigma^2 + 2\eta|\mu| + \lambda + x + 2\lambda\eta|p\eta - q\theta| + \lambda\eta\theta$, and $Y_4 = \frac{Y_3}{\eta\theta}$.

PROOF. For any fixed $x > 0$ and any $y \in \mathbb{R}$, the equation $G(z) = x + iy$ has exactly four complex roots, $\beta_{1,x+iy}$, $\beta_{2,x+iy}$, $\gamma_{1,x+iy}$ and $\gamma_{2,x+iy}$, which are all continuous functions of y (see, e.g., Ostrowski [22]). In particular, when $y = 0$, Kou and Wang [19] showed that all the four roots are real and satisfy

$$-\infty < \gamma_{2,x} < -\theta < \gamma_{1,x} < 0 < \beta_{1,x} < \eta < \beta_{2,x} < +\infty. \tag{35}$$

We claim that for the fixed $x > 0$ and any $y \in \mathbb{R}$, the real parts of the four complex roots are all non-zero. Otherwise, there exist $d, y \in \mathbb{R}$ such that $G(id) = x + iy$. However, this contradicts to

$$\begin{aligned}\Re(G(id)) &\le -\frac{\sigma^2}{2}d^2 - \lambda + \lambda\left|\frac{p\eta}{\eta - id}\right| + \lambda\left|\frac{q\theta}{\theta + id}\right| \le -\frac{\sigma^2}{2}d^2 - \lambda + \lambda p + \lambda q \\ &= -\frac{\sigma^2}{2}d^2 \le 0 < x.\end{aligned}$$

Note that the real parts of the four roots are all continuous in y. Moreover, by (35) we know $\Re(\beta_{j,x+iy}) > 0$ and $\Re(\gamma_{j,x+iy}) < 0$ for $j = 1, 2$ when $x > 0$ and $y = 0$. Therefore, this still holds for the fixed $x > 0$ and any $y \in \mathbb{R}$, i.e., there exists exactly two roots with positive real parts.

Now we begin to prove (34). For the first inequality in (34), define

$$f_1(z) := (\eta - z)(\theta + z), \quad g_1(z) := \frac{\lambda((p\eta - q\theta)z + \eta\theta)}{\frac{1}{2}\sigma^2 z^2 + \mu z - \lambda - x - iy},$$

and a disk $K_1 := \{z \in \mathbb{C} : |z - \eta| < R_1\}$ with $R_1 = \frac{Y_3}{|y|\theta} < \eta$ (because $|y| > Y_4$). Thus for all $z \in \overline{K_1}$, we have $\Re(z) > 0$ and $|z| < 2\eta$. Then for any

$z \in \overline{K_1}$ and $|y| > Y(x)$, the denominator of $g_1(Z)$ must be non-zero because its absolute value satisfies

$$\left|\frac{1}{2}\sigma^2 z^2 + \mu z - \lambda - x - iy\right| \geq |iy| - \left|\frac{1}{2}\sigma^2 z^2 + \mu z - \lambda - x\right| \geq |y| - 2\eta^2\sigma^2 - 2\eta|\mu| - \lambda - x > 0. \tag{36}$$

Here the second inequality holds because $|z| < 2\eta$ and the last holds because $|y| > Y(x) \geq Y_3$. Therefore, $g_1(z)$ is analytic on $\overline{K_1}$. Furthermore, by (36) we can obtain that for any $z \in \partial K_1$ and $|y| > Y(x)$,

$$|g_1(z)| \leq \frac{|\lambda(p\eta - q\theta)z + \lambda\eta\theta|}{|y| - 2\eta^2\sigma^2 - 2\eta|\mu| - \lambda - x} \leq \frac{2\lambda\eta|p\eta - q\theta| + \lambda\eta\theta}{|y| - 2\eta^2\sigma^2 - 2\eta|\mu| - \lambda - x} =: \frac{h_1(|y|)}{|y|}, \tag{37}$$

where $h_1(u) := \frac{(2\lambda\eta|p\eta - q\theta| + \lambda\eta\theta)u}{u - 2\eta^2\sigma^2 - 2\eta|\mu| - \lambda - x}$ is decreasing in u for $u > Y_3$. It follows from (37) that

$$|g_1(z)| \leq \frac{h_1(|y|)}{|y|} \leq \frac{h_1(Y_3)}{|y|} = \frac{Y_3}{|y|} = R_1\theta, \quad \text{for any } z \in \partial K_1 \text{ and } |y| > Y(x).$$

On the other hand, apparently $f_1(z)$ is analytic on $\overline{K_1}$. Moreover, since $\Re(z) > 0$ and $\theta > 0$, we have

$$|f_1(z)| = R_1|\theta + z| > R_1\theta, \text{ for any } z \in \partial K_1.$$

Thus Rouché's Theorem applies and implies that for any $|y| > Y(x)$, the number of zeros of $f_1(z) + g_1(z)$ in K_1 is the same as that of $f_1(z)$ in K_1. Hence for any $|y| > Y(x)$, $G(z) = x + iy$ has exactly one root in K_1 because $G(z) - (x + iy) \equiv \frac{\frac{1}{2}\sigma^2 z^2 + \mu z - \lambda - x - iy}{(\eta - z)(\theta + z)} \cdot [f_1(z) + g_1(z)]$. The first inequality in (34) is proved.

The second inequality in (34) can be proved via Rouché's Theorem analogously with $f_2(z) := \frac{1}{2}\sigma^2 z^2 - iy$, $g_2(z) := \lambda(\frac{p\eta}{\eta - z} + \frac{q\theta}{\theta + z} - 1) - x + \mu z$, and a disk $K_2 := \{z \in \mathbb{C} : |z - z_y| < \frac{2|\mu|}{\sigma^2}\}$. The length proof is omitted and available upon request. □

LEMMA G.3. *$L_f(\vec{s})$ satisfies (13) except that $\alpha_1 = \alpha_3 = 1$, $\alpha_2 = \alpha_4 = 0$, $M_1 = Y(v_1)$, $M_2 = 1$,*

$$\zeta_1(\vec{v}, \omega_1) = e^{-bv_2}\left(\left|\frac{e^{-b\beta_{1,s_1}}(\eta - \beta_{1,s_1}) + e^{-b\beta_{2,s_1}}(\beta_{2,s_1} - \eta)}{\beta_{2,s_1} - \beta_{1,s_1}}\right|\right.$$

$$+\frac{|(e^{-b\beta_{1,s_1}}-e^{-b\beta_{2,s_1}})(\beta_{2,s_1}-\eta)(\eta-\beta_{1,s_1})|}{|\beta_{2,s_1}-\beta_{1,s_1}|\cdot(\eta+v_2)}\Big),$$

$$\zeta_2(\vec{v},\omega_2)=\frac{e^{-bv_2}}{T_0}(T_1+T_2+T_3),\ \textit{and}\ \zeta(\vec{v})=\zeta_2(\vec{v},0),$$

where

$$T_0=|z_{M_1}-\eta|-\frac{Y_3}{M_1\theta}-\frac{2|\mu|}{\sigma^2},\quad T_1=e^{-b\left(\eta-\frac{Y_3}{M_1\theta}\right)}\frac{Y_3}{\theta},$$

$$T_2=\frac{16\sigma^2}{b^2}e^{-\frac{b}{2}\left(\frac{\sqrt{|\omega_1|}}{\sigma}-\frac{2|\mu|}{\sigma^2}\right)}\left(|z_{M_1}-\eta|-\frac{2|\mu|}{\sigma^2}\right),$$

$$T_3=\frac{Y_3}{\theta|\eta+s_2|}\left[e^{-b\left(\eta-\frac{Y_3}{M_1\theta}\right)}+e^{-b\left(\frac{\sqrt{M_1}}{\sigma}-\frac{2|\mu|}{\sigma^2}\right)}\right]\left(|z_{M_1}-\eta|-\frac{2|\mu|}{\sigma^2}\right),$$

$z_{M_1}=\frac{\sqrt{M_1}}{\sigma}(1+i\cdot sgn(\omega_1))$, *and* $Y(\cdot)$, Y_3, β_{1,s_1} *and* β_{2,s_1} *are the same as in Lemma G.2.*

Proof. By (24) we obtain $|L_f(\vec{s})|\le\zeta_1(\vec{v},\omega_1)$. Hence for all $\vec{\omega}$, in particular, for all $\vec{\omega}\in D_2^{\vec{M}}$, we have $|L_f(\vec{s})|\le\zeta_1(\vec{v},\omega_1)\equiv\zeta_1(\vec{v},\omega_1)|\omega_2|^{-\alpha_2}$.

When $\vec{\omega}\in D_1^{\vec{M}}\cup D_3^{\vec{M}}\equiv\{\vec{\omega}:|\omega_1|>M_1\}$, we have $|\omega_1|>Y(v_1)$. Thus applying Lemma G.2 yields

$$|e^{-b\beta_{1,s_1}}|=e^{-b\Re(\beta_{1,s_1})}\le e^{-b\left(\eta-\frac{Y_3}{M_1\theta}\right)}$$

$$|e^{-b\beta_{2,s_1}}|=e^{-b\Re(\beta_{2,s_1})}\le e^{-b\left(\frac{\sqrt{|\omega_1|}}{\sigma}-\frac{2|\mu|}{\sigma^2}\right)}. \tag{38}$$

Moreover, when $\vec{\omega}\in D_1^{\vec{M}}\cup D_3^{\vec{M}}$, from the definition of $Y(\cdot)$ in Lemma G.2 we conclude that $|\omega_1|>Y(v_1)\ge Y_1\equiv 2(\sigma\eta+\frac{2|\mu|}{\sigma})^2$, which further implies $\Re(z_{\omega_1})-\frac{2|\mu|}{\sigma^2}>\Re(z_{M_1})-\frac{2|\mu|}{\sigma^2}=\frac{\sqrt{|M_1|}}{\sigma}-\frac{2|\mu|}{\sigma^2}>\frac{\sqrt{Y_1}}{\sigma}-\frac{2|\mu|}{\sigma^2}\ge\eta$. It follows that $|z_{\omega_1}-\eta|\ge|z_{M_1}-\eta|$. Therefore, for any $\vec{\omega}\in D_1^{\vec{M}}\cup D_3^{\vec{M}}$,

$$\begin{aligned}I_1(\omega_1):=|\beta_{2,s_1}-\beta_{1,s_1}|&\ge|z_{\omega_1}-\eta|-|z_{\omega_1}-\beta_{2,s_1}|-|\beta_{1,s_1}-\eta|\\&\ge|z_{M_1}-\eta|-|z_{\omega_1}-\beta_{2,s_1}|-|\beta_{1,s_1}-\eta|\\&\ge|z_{M_1}-\eta|-\frac{2|\mu|}{\sigma^2}-\frac{Y_3}{M_1\theta},\end{aligned} \tag{39}$$

where the last inequality holds due to Lemma G.2. Furthermore, for any $\vec{\omega}\in D_1^{\vec{M}}\cup D_3^{\vec{M}}$, we have

$$I_2(\omega_1):=\left|\frac{\beta_{2,s_1}-\eta}{\beta_{2,s_1}-\beta_{1,s_1}}\right|\le 1+\left|\frac{\beta_{1,s_1}-\eta}{\beta_{2,s_1}-\beta_{1,s_1}}\right|$$

$$\leq 1+\frac{\frac{Y_3}{M_1\theta}}{|z_{M_1}-\eta|-\frac{2|\mu|}{\sigma^2}-\frac{Y_3}{M_1\theta}}=\frac{|z_{M_1}-\eta|-\frac{2|\mu|}{\sigma^2}}{|z_{M_1}-\eta|-\frac{2|\mu|}{\sigma^2}-\frac{Y_3}{M_1\theta}}, \tag{40}$$

where the second inequality holds because of Lemma G.2 and (39). Besides, define $h(x) := xe^{-\frac{b}{2\sigma}\sqrt{x}}$ for $x \geq 0$. It is easy to obtain that $h(x)$ attains its maximum at $x = 16\sigma^2/b^2$.Thus by (38) we have

(41)

$$I_3(\omega_1) := |\omega_1 e^{-\frac{b}{2}\beta_{2,s_1}}| \leq |\omega_1| e^{-\frac{b}{2\sigma}\sqrt{|\omega_1|}+\frac{b|\mu|}{\sigma^2}} \leq h\left(\frac{16\sigma^2}{b^2}\right) e^{\frac{b|\mu|}{\sigma^2}} < \frac{16\sigma^2}{b^2} e^{\frac{b|\mu|}{\sigma^2}}.$$

From (24) we obtain

$$\begin{aligned}|L_f(\vec{s})| \leq e^{-bv_2}\Big\{&e^{-b\beta_{1,s_1}}|\eta-\beta_{1,s_1}|/I_1(\omega_1)+e^{-\frac{b}{2}\beta_{2,s_1}}I_2(\omega_1)I_3(\omega_1)/|\omega_1|\\&+[(e^{-b\beta_{1,s_1}}+e^{-b\beta_{2,s_1}})|\eta-\beta_{1,s_1}|I_2(\omega_1)]/|\eta+s_2|\Big\}\end{aligned}$$

Substituting (34), (38), (39), (40) and (41) into the RHS of the inequality above yields $|L_f(\vec{s})| \leq \frac{\zeta_2(\vec{v},\omega_2)}{|\omega_1|} \leq \frac{\zeta(\vec{v})}{|\omega_1|}$ for all $\vec{\omega} \in D_1^{\vec{M}} \cup D_3^{\vec{M}}$. □

Proof of Proposition 6.2. For any $\vec{v} \in$ ROAC of $L_f(\vec{s})$, from Table 4 we know

$$\begin{aligned}|L_F(s_1,-s_2)| &= \left|\frac{1}{-s_2(s_1-G(-s_2))}L_f(\vec{s})\right| \\ &\leq \frac{1}{|\omega_2|}\frac{1}{|s_1-G(-s_2)|}\cdot|L_f(\vec{s})|\end{aligned} \tag{42}$$

$$\begin{aligned}|L_{\mathrm{UIC}}(s_1-r,-s_2-1)| &= \left|\frac{S_0^{-s_2}}{-s_2(-s_2+1)(s_1-G(-s_2))}L_f(\vec{s})\right| \\ &\leq \frac{S_0^{-v_2}}{|\omega_2|^2}\left|\frac{1}{s_1-G(-s_2)}\right|\cdot|L_f(\vec{s})|.\end{aligned} \tag{43}$$

Combining Lemma G.1 and G.3 with (42) yields

$$|L_F(s_1,-s_2)| \leq \begin{cases}\hat{\zeta}^{-1}\zeta_2(\vec{v},\omega_2)|\omega_1|^{-2}, & \text{for all } \vec{\omega} \in D_1^{\vec{M}^F};\\ 4\sigma^{-2}\zeta_1(\vec{v},\omega_1)|\omega_2|^{-3}, & \text{for all } \vec{\omega} \in D_2^{\vec{M}^F};\\ 2\sigma^{-1}\zeta(\vec{v})|\omega_1|^{-\frac{3}{2}}|\omega_2|^{-2}, & \text{for all } \vec{\omega} \in D_3^{\vec{M}^F},\end{cases} \tag{44}$$

where $\vec{M}^F := (M_1^F, M_2^F)$ with $M_j^F = \max\{M_j^*, M_j\}$ for $j = 1, 2$. Here, M_1^*, M_2^*, and $\hat{\zeta}$ are given in Lemma G.1 with v_2 replaced by $-v_2$, while M_1, M_2, $\zeta_1(\vec{v},\omega_1)$, $\zeta_2(\vec{v},\omega_2)$, and $\zeta(\vec{v})$ are given in Lemma G.3.

Similarly, combining Lemma G.1 and G.3 with (43) yields

(45)
$$|L_{\mathrm{UIC}}(s_1 - r, -s_2 - 1)| \leq \begin{cases} \hat{\zeta}^{-1} S_0^{-v_2} \zeta_2(\vec{v}, \omega_2) |\omega_1|^{-2}, \text{ for all } \vec{\omega} \in D_1^{\vec{M}^{UIC}}; \\ 4\sigma^{-2} S_0^{-v_2} \zeta_1(\vec{v}, \omega_1) |\omega_2|^{-4}, \text{ for all } \vec{\omega} \in D_2^{\vec{M}^{UIC}}; \\ 2\sigma^{-1} S_0^{-v_2} \zeta(\vec{v}) |\omega_1|^{-\frac{3}{2}} |\omega_2|^{-3}, \text{ for all } \vec{\omega} \in D_3^{\vec{M}^{UIC}}, \end{cases}$$

where $\vec{M}^{UIC} \equiv \vec{M}^F$. The proof of Proposition 6.2 is completed. □

REFERENCES

[1] Abate, J. and Whitt, W. (1992). The Fourier-series method for inverting transforms of probability distributions. *Queueing Systems* **10**(1–2) 5–88. MR1149995

[2] Broadie, M. and Yamamoto, Y. (2003). Application of the fast Gaussian transform to option pricing. *Management Science* **49**(8) 1071–1088.

[3] Brychkov, Y., Glaeske, H., Prudnikov, A. and Tuan, V. (1992). *Multidimensional Integral Transformations.* Gordon and Breach Science Publishers. MR1177594

[4] Cai, N., Chen, N. and Wan, X. (2010). Occupation times of jump-diffusion processes with double-exponential jumps and the pricing of options. *Mathematics of Operations Research* **35**(2) 412–437. MR2674727

[5] Cai, N. and Kou, S. G. (2011). Option pricing under a mixed-exponential jump diffusion model. *Management Science* **57**(11) 2067–2081.

[6] Cai, N. and Kou, S. G. (2012). Pricing Asian options under a hyper-exponential jump diffusion model. *Operations Research* **60**(1) 64–77. MR2911657

[7] Cai, N., Kou, S. G. and Liu, Z. 2014. A two-sided Laplace inversion algorithm with computable error bounds and its application in financial engineering. *Advances in Applied Probability* **46**(3) 766–789. MR3254341

[8] Cai, N. and Sun, L. 2014. Valuation of stock loans with jump risk. *Journal of Economic Dynamics and Control* **40**(3) 213–241. MR3166501

[9] Carr, P. and Madan, D. B. 1999. Option valuation using the fast Fourier transform. *Journal of Computational Finance* **2**(4) 61–73.

[10] Carr, P. and Madan, D. B. (2009). Saddlepoint methods for option pricing. *Journal of Computational Finance* **13**(1) 49–61. MR2557532

[11] Choudhury, G. L., Lucantoni, D. M. and Whitt, W. (1994). Multidimensional transform inversion with applications to the transient M/G/1 queue. *Annals of Applied Probability* **4**(3) 719–740. MR1284982

[12] Feng, L. and Lin, X. (2013). Inverting analytic characteristic functions and financial applications. *SIAM Journal on Financial Mathematics* **4**(1) 372–398. MR3054585

[13] Feng, L. and Linetsky, V. (2008). Pricing discretely monitored barrier options and defaultable bonds in Lévy process models: A fast Hilbert transform approach. *Mathmatical Finance* **18**(3) 337–384. MR2427727

[14] Feng, L. and Linetsky, V. (2009). Computing exponential moments of the discrete maximum of a Lévy process and lookback options. *Finance and Stochastics* **13**(4) 501–529. MR2519842

[15] Glasserman, P. and Liu, Z. (2010). Sensitivity estimates from characteristic functions. *Operations Research* **58**(6) 1611–1623. MR2752708

[16] Grafakos, L. (2004). *Classical and Modern Fourier Analysis.* Pearson Education, Inc. MR2449250

[17] Hurd, T. R. and Zhou, Z. (2010). A Fourier transform method for spread option pricing. *SIAM Journal on Financial Mathematics* **1**(1) 142–157. MR2592568

[18] Kou, S. G. (2002). A jump-diffusion model for option pricing. *Management Science* **48**(8) 1086–1101.

[19] Kou, S. G. and Wang, H. (2003). First passage times for a jump diffusion process. *Advances in Applied Probability* **35** 504–531. MR1970485

[20] Kou, S. G., Petrella, G. and Wang, H. (2005). Pricing path-dependent options with jump risk via Laplace transforms. *Kyoto Economic Review* **74** 1–23.

[21] Lee, R. (2004). Option pricing by transform methods: Extensions, unification, and error control. *Journal of Computational Finance* **7**(3) 51–86.

[22] Ostrowski, A. (1940). Recherches sur la méthode de Graeffe et les zéros des polynomes et des séries de Laurent. *Acta Mathematica* **72**.

[23] Petrella, G. (2004). An extension of the Euler Laplace transform inversion algorithm with applications in option pricing. *Operations Research Letters* **32**(4) 380–389. MR2057794

[24] Rogers, L. C. G. (2000). Evaluating first-passage probabilities for spectrally one-sided Lévy processes. *Journal of Applied Probability* **37**(4) 1173–1180. MR1808924

[25] Schiff, J. (1999). *The Laplace Transform: Theory and Applications.* Springer. MR1716143

[26] Valkó, P. and Abate, J. (2005). Numerical inversion of 2-D Laplace transforms applied to fractional diffusion equations. *Applied Numerical Mathematics* **53**(1) 73–88. MR2124002

Ning Cai
Room 5521, Academic Building
HKUST, Clear Water Bay
Kowloon, Hong Kong, China
E-mail: ningcai@ust.hk

Chao Shi
Room 708, Boxue Building
10 East Huixin Street, Chaoyang District
Beijing, China
E-mail: shichao@ust.hk